Inference accuracy about an aircraft crash

François Graner*
Université Paris Cité, CNRS, Matière et Systèmes Complexes, Paris, France.

Stefano Matthias Panebianco†
Université Paris-Saclay, Centre d'Etudes de Saclay (CEA), IRFU, Département de Physique Nucléaire (DPhN), Saclay, France
(Dated: July 5, 2025)

Problem-based learning benefits from situations taken from real life, which arouse student interest. The shooting of Rwanda president aircraft on April 6th, 1994 is still unsolved. We discuss the methods to infer information and conclusions about where the aircraft was shot and its trajectory during its fall, as well as about the place from which the missiles were launched, and their trajectory and type. To this goal, we compiled expert reports, witness indications and other public sources, then translated plain language sentences into quantitative equalities and inequalities applied to geometry and mechanics at undergraduate level. The accuracy of each result is discussed and propagated in order to ensure a proper assessment of the hypotheses and a traceability of their consequences. Overall, the accuracy discussion can train the students critical mind, and teach inference methods which are routinely used in several fields of physics research. In addition, it demonstrates the importance and limits of scientific expertise during a judiciary process. The publicly available information interpreted by our calculations shows that the question of missile launching position is still open.

I. INTRODUCTION

A. Motivation and approach

1. Motivation

Daily life physics is an endless source for problem-based learning. Students have to list questions relevant to physics, find existing information, extract and interpret raw data, and compensate for missing data. They then need to identify which domains of physics play a role in the analysis, translate plain language sentences into equalities or inequalities suitable for quantitative data handling, make hypotheses and critically discuss them. Next, they should aggregate indications which are inaccurate and sometimes incompatible, distinguish which information constrains the results and which does not, deal with an under- or over-constrained set of equations, and eventually determine the accuracy of the final result.

In particular, forensic physics is taught in several undergraduate courses (see a list in Ref.[1]), and involves several fields of physics[2]. A consultant in forensics explains: "I see students' interest click when I bring in real-life cases"; he adds that the physics tends to be straightforward but the application requires some subtlety[3]. Examples include gunshot location through recorded sound[4].

Choosing a case with a consensus on all data ("solved" case) would have the advantage to enable validation of student findings. Here, on the opposite, we chose an unsolved case, which adds some mystery and interest to the study. We examined an historically important aircraft crash for which information is only partially available, and undergraduate level calculations can help bridging the gaps to determine where (and from where) the aircraft was shot by a missile. We contribute to solve the "where" question, and explain why the "from where" question is still unsolved.

2. Approach

We consulted several sources on the internet as available in early 2024 (except when noted otherwise), including expert reports regarding aeronautics, weapons, ballistics or radio communications, as well as on-site measurements and tens of witness indications. We reexamined the available information within a problem-based learning approach, inferring results, and critically discussing the methodology. Witness indications can be subjective, imprecise, or contradictory due to memory distortions. At two occurrences (Sections III A, IV B) we noted that a witness provided, at few years interval, depositions which differed (lack of stability in time). For each section, we selected the witness indications which provided exploitable information; depending on their number we treated them either statistically, or individually.

We refer the reader to Table III which is a guide through the details of the paper. We rewrote the raw data in a quantitative form accessible to students, homogeneized using SI units. We tried to accurately determine, combine and trace the uncertainty sources[5]; for that purpose, rather than directly working on a map we chose to work with suitably defined cartesian coordinates (and we later drew the results on a map, which was an additional source of inaccuracy). In order to avoid propagation of rounding errors discussed in Section V B 1, we kept digits in excess throughout all calculations; we rounded the results only in Section V B 2. Whenever possible we used the word "accuracy", rather than "uncertainty" which in general audiences is perceived as ambiguous and generating mistrust[3]. Unless explicitly stated, we used the sign $\pm$ to refer to the possible discrepancy between the value we estimate and the unknown true one.

B. Context and facts

1. The event

The shooting of Falcon 50 aircraft registered as 9XR-NN (Fig. 1) in Rwanda on April 6th, 1994 was a dramatic event. The aircraft owner Juvénal Habyarimana, president of Rwanda, and his guest Cyprien Ntaryamira, president of Burundi, had spent the day in Dar-Es-Salaam (Tanzania) for a regional summit. In the evening, with 7 other passengers and 3 crew members, their aircraft had almost finished its descent and deceleration, and was arriving at a few kilometers of Kigali airport, when it was shot by a missile. All 12 persons died in the crash. Within a day, Rwandan army units and extremist Hutu militias began to perpetrate the Tutsi genocide on a large scale. Much

(a) (b)

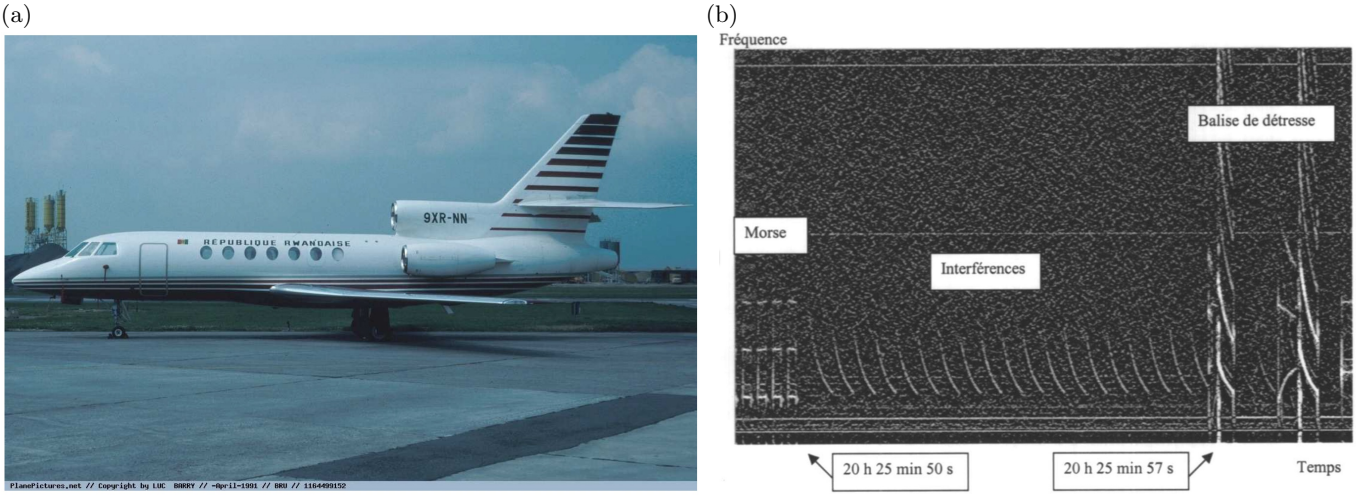

FIG. 1. **The aircraft and its publicly available signals recorded by the airport.** (a) Dassault Falcon 50 aircraft photographed in April 1991 at Bruxelles - Zaventem airport. PlanePictures.net - Copyright by Luc Barry - April 1991 - BRU - 1164499152, quoted in Ref.[9] p. 7. (b) Ten seconds of radio signals emitted by the aircraft, selected by the French aircraft crash expert, who has added labels in french (Ref.[8] p. 13). Translation: "Fréquence" = frequency, "Temps" = time, "Balise de détresse" = distress beacon, "Morse" = signal similar to Morse alphabet, "Interférences" = interferences.

information on the aircraft crash is inaccessible due in particular to the murder of thousands of witnesses, lack of flight recorder data, and disparition of several airport records.

2. Sources

Several documents are available online on aeronautic or military websites and on the database `francegenocidetutsi.org`. French military investigators have searched the aircraft during the night after the crash, and the French justice has proceeded with witness hearings[6]. In spring and summer 1994, Belgian military investigators questioned witnesses, and on August 1st two of them examined the aircraft fragments remaining on site[7]. On April 10th, 2002 a French aircraft crash expert issued an analysis of some air traffic control recordings[8]. A seven-members Rwandan commission has heard 577 witnesses from February 2008 to February 2009, has commissionned two UK military experts (ammunitions, forensic) who have issued their report[9] on February 27th, 2009, then published its own final report in April 20th, 2009[10] along with a brief synopsis in video[11]. On January 5th, 2012 was published the report of a group of six French experts: aviation, ballistics, weapons, explosives and land survey[12] complemented by acoustics[13].

Exploiting the sources raised a few technical difficulties. We convert in SI units the aeronautic units: a foot is 0.3048 m, a mile is 1852 m, a knot is 0.514 m/s, a dot is 0.5° or 8.7 10^{-3} rad. We count anticlockwise angles as positive, i.e. with the trigonometric convention (rather than with the compass convention, clockwise). Aeronautic maps use the magnetic North; the difference with geographic North (the "declination") was 3° West for the 1999 map (Ref.[12] p. 185), 0° for the 2006 one (Ref.[9] p. 106), 1° East for the 2024 one[14], so that the direction of the airport track (called "runway 28") was marked as 77°, 80° or 81°, respectively. We consistently use the geographic North, so that the runway orientation is 80° whatever the year.

Kigali international Airport (IATA code: KGL; ICAO code: HRYR), sometimes referred to as Kanombe International Airport, and at that time called Grégoire Kayibanda international airport, is located in Kanombe, in the eastern suburbs of the Rwanda capital Kigali. The altitude z of runway 28 threshold O (east end) is $z_O = 1486$ m above sea level (4874 feet[14]). We take O as the origin for both horizontal axes: axis Ox, along the runway, oriented positively from West to East, and axis Oy, perpendicular to the runway, oriented from South to North (Fig. 2).

According to the standard instrument approach procedure, an aircraft is expected to follow a well-defined trajectory

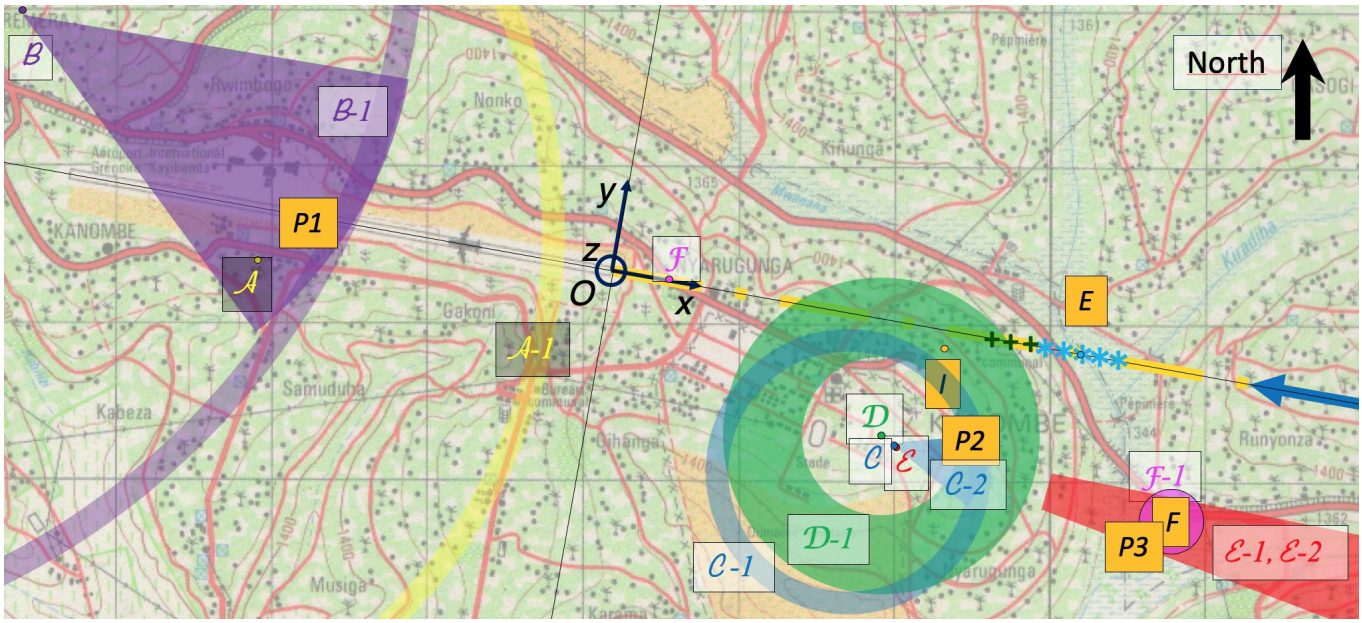

FIG. 2. **Distance indications on missile-aircraft encounter and missile launching place.** Geographic North is towards the top (thick black arrow). Scale: grid size is 1 km; the length of the airport runway (barely visible on the top left) is 3500 m[14]. At that date the airport was outside of Kigali city, which is off the left of this map. Thick yellow dash-dotted line indicates the standard aircraft trajectory along the Ox axis, and the thick blue arrow is the direction of aircraft arrival; the crew announcement position A and glide interception G are off the right of this image. Witness positions and their indications were measured by us using the reference map established by French investigators (Ref.[13], Annex C), then overlaid by us on a 1988 map[17], copyright IGN Brussels (paper version scanned by us at 4800 dpi resolution). I marks the aircraft impact on the ground (orange dot). Witnesses are labeled by letters (ex: $\mathcal{A}$), their positions are labeled by coloured dots, their indications are labeled by a number (ex: $\mathcal{A}$*–1*). *Witness indications regarding missile-aircraft encounter position E (Section II D).* The blue dot marks E and the five blue stars ($*$) mark its confidence interval, estimated backwards from the impact data. The three dark green crosses ($+$) mark the position of E (and its confidence interval) which would be estimated under the assumption of free fall detailed in Section II C. *Witness indications regarding distance to missile launching place (Section III A).* Witness indications of distance are based on sound, and are combined with their direction indications whenever available. Boundary of possible missile launching positions using Eq. (6) and assuming the missile Mach number is of order 2 (Section IV C): pale yellow circle, according to $\mathcal{A}$*–1* ($\mathcal{A}$ does not provide direction indication); pale purple circle, according to $\mathcal{B}$*–1* ($\mathcal{B}$ broadly indicates the direction of the airport, see pale purple angular sector); pale blue circle, according to $\mathcal{C}$*–1* ($\mathcal{B}$ indicates the direction of Masaka, see pale blue angular sector $\mathcal{C}$*–2*). Since $\mathcal{D}$ indicates an interval between 500 and 1000 m ($\mathcal{D}$*–1*) and no direction, we drew an annulus (pale green) centered around $\mathcal{D}$'s house. Since $\mathcal{E}$ was at $\mathcal{C}$'s house, indicates an interval between 1000 to 5000 m ($\mathcal{E}$*–1*) and precisely indicates the direction of Masaka valley ($\mathcal{E}$*–2*), we drew a truncated angular sector originating from $\mathcal{C}$'s house (pale red). F is the factory (called "Guttanit") indicated by $\mathcal{F}$*–1* and the fuschia circle is its confidence interval. "$P1$", "$P2$" and "$P3$" mark Pair 1 (broad intersection of $\mathcal{A}$*–1* and $\mathcal{B}$*–1*), Pair 2 (intersection of $\mathcal{C}$*–1*/$\mathcal{C}$*–2* and $\mathcal{D}$*–1*), and Pair 3 (intersection of $\mathcal{E}$*–1*/$\mathcal{E}$*–2* and $\mathcal{F}$*–1*), respectively.

(Fig. 3) in the vertical Oxz plane, at an angle $\gamma = 3.00°$ from the horizontal, called the "glide":

$$y = 0 \tag{1}$$

$$z = z_O + x \tan\gamma = 1486 + 0.052\, x \tag{2}$$

This prescribed trajectory starts at 7.8 miles (Ref.[9] p. 106) i.e. at $x_G = 14446$ m. It ends exactly at the runway threshold O. Seen from O, its angular accuracy both in y and in $z - z_O$ is $\pm$ 1 dot[15,16], or $\pm 8.7\ 10^{-3}$ rad. Hence we retain a linear accuracy $\pm 8.7\ 10^{-3}\ x$ on the value of both y and $z - z_O$.

3. *Crash data*

According to the few available recorded conversations between the pilots and the air traffic controllers[8], the crew announced at t_A = 20h21'27" that the aircraft was at 20 miles (x_A= 37040 m) and 12000 ft altitude (z_A = 3657 m). At 20h21'42", it asked to make a direct approach into runway 28. The controller informed the aircraft (Ref.[8] p. 11)

that wind speed was 2.06 m/s (4 knots), temperature was 19°C, ceiling and visibility were OK ("CAVOK"). More than two hours after sunset, it was dark night. All witnesses agree that the sky was clear and dark, without significant wind.

Around 20h26', the aircraft had already begun to descend towards the airport. Most witnesses saw two successive luminous lines coming from the South side of the aircraft; the first one came close to the aircraft and missed it, the second one encountered the aircraft. The witnesses' indications do not determinate the actual action, i.e. whether the missile hit the aircraft or exploded near it, for instance. Section IV discusses whether these were missile trajectories, and whether there were actually two of them.

After a few seconds, a big fireball was visible while the aircraft fell. Machine guns close to the airport shot, including with tracer bullets. The aircraft hit the ground, bounced, and got dislocated. It eventually hit (and punched through) the wall of the President's residence, located close to the airport and (by mere coincidence) home of the aircraft owner. The combination of a fireball, the presence of two presidents, the crash in the aircraft owner's residence, and the subsequent historical events, have all contributed to dramatise this crash. However, the trajectory of the aircraft was normal almost until its end, the aircraft was already low and slow, it narrowly missed the runway threshold, and most of it was intact until it hit the ground.

The airport detected a signal on the distress frequency during a 22 seconds time interval, between 20h25'50" and 20h26'12" (Ref.[8] p. 10-13). The French aircraft crash expert assumed this whole time interval was the time of the crash (Ref.[8] p. 12) i.e. did not distinguish between the time of the aircraft-missile encounter, t_E, versus that of the aircraft impact on the ground, t_I. In fact, the signal was too unusual to be attributed to any precise event: it superimposed two components of unknown origin (Fig. 1b). The first component was perceived during the whole 22 s interval; on Fig. 1b we can see 7 s of it, with 19 evenly spaced occurrences, hence we determine its period was 0.37 ± 0.05 s; the expert labeled it as "interferences" without specific justifications. The second component was perceived with 5 evenly spaced occurrences, at 20h25'57", 20h25'59", 20h26'02", 20h26'05" and 20h26'07" (see details in Ref.[8] p. 10, 12), hence we determine its period is 2.50 ± 0.25 s. The expert showed only its first occurrence, marked "20 h 25 min 57 s", and its second one, unmarked (Fig. 1b). It was termed "distress beacon" by the expert, although it did not emit after 20h26'12", while in principle once activated (manually or due to a shock) a distress beacon is built to emit over days. We leave these signals open for interpretation. Given the lack of information, we globally retain that t_E and t_I were probably close to each other, both being around 20h26'01" ± 11 s. We anticipate that their difference $D = t_I - t_E$ was approximately ten seconds and we will come back to that point in Sections II C, II D.

The aircraft impact position I on the ground is known (Fig. 2). The impact trace was visible in 1994 as a 8 m circle, hence its position has been determined with a few meters accuracy by Belgian investigators, as well as that of several aircraft fragments dispersed over a rectangle (Fig. 3a) of 145 m × 20 m (Ref.[7] p. 5). Over the years, several fragments have been moved, degraded or removed, as described and mapped with laser range finding equipment in 2009 by UK experts (Ref.[9] p. 8). In 2012, French investigators combined their own geometrical measurements with the 1994 Belgian report to determine within a few meters the impact position I coordinates as $x_I = 2160$ m, $y_I = -100$ m and $z_I = 1410$ m (Ref.[12] p. 188, 192).

II. ENCOUNTER POSITION

The aircraft-missile encounter position E is not known. Finding it requires several steps, for instance to infer it from the impact position I by reverse analysis of the aircraft trajectory between the encounter and the impact (Sections II C, II D). This is possible since we first determine the aircraft longitudinal speed $\dot{x}$ (hereafter "speed", for short, and the dot indicates the time derivative) and its direction at the time of the encounter and at the time of impact (Sections II A, II B).

A. Aircraft speed as a function of time

To determine the velocity vector as a function of time or position, it is first useful to determine to which extent the aircraft velocity vector differs (Fig. 3) just after encounter ($t > t_E$) from just before encounter ($t < t_E$). While the aircraft position was necessarily continuous, a change in velocity vector could arise from several possible ingredients.

Momentum transfer from the missile itself was possible if the missile actually hit the aircraft. The modification of the aircraft *velocity vector* was oriented from South to North and bottom-up, see short red arrows on Fig. 3 (for the modification of the aircraft *angular velocity* see Section II B). Its magnitude depended on both the impact place and impact direction. We estimate an upper bound on its magnitude as follows. The order of magnitude of the aircraft mass M with fuel and passengers was larger than 10^4 kg (when empty, its mass is 9163 kg[18]). A missile considered here (Section IV C) has a mass m of order of at most 20 kg and a speed at most 1000 m/s[12]. The mass ratio m/M was

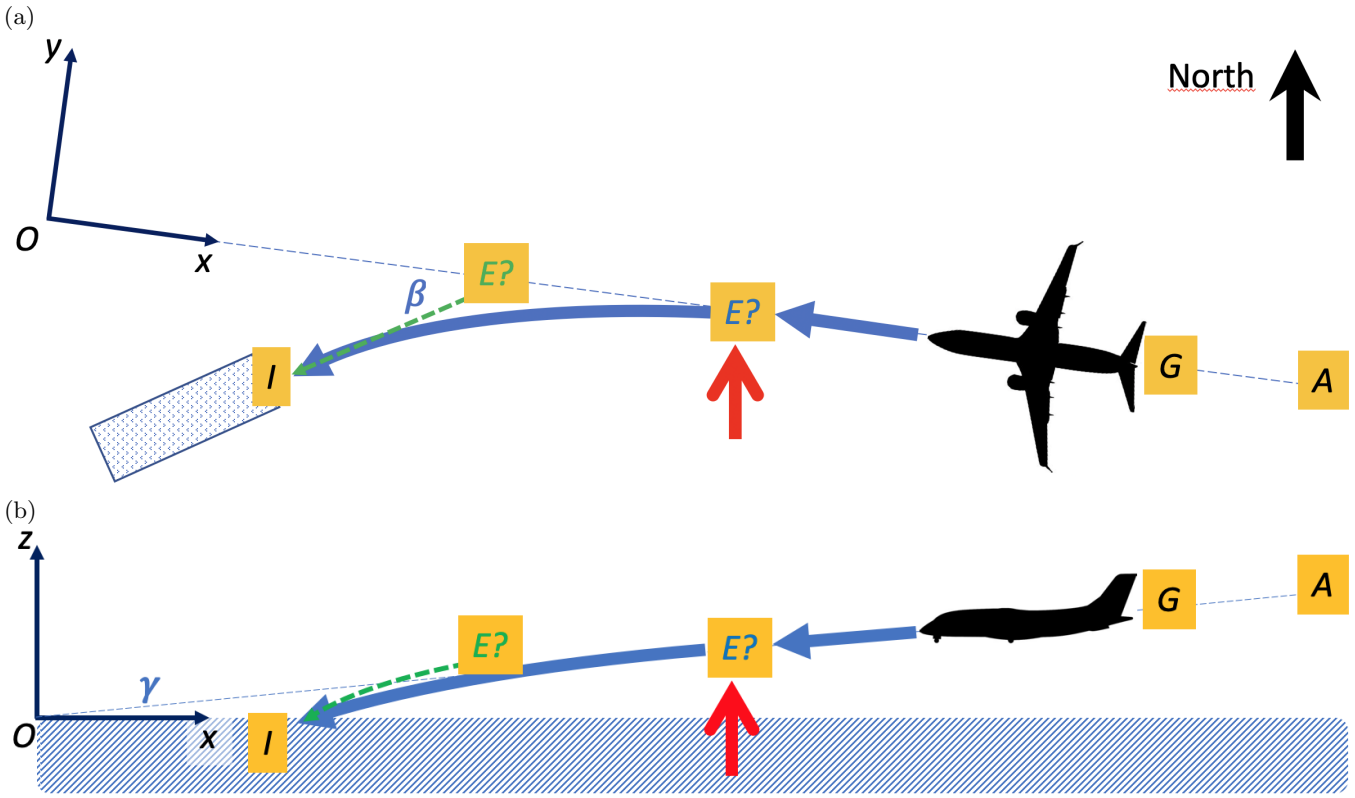

FIG. 3. **Schema (not to scale) of the aircraft velocity vectors before and after missile-aircraft encounter E.** We know aircraft positions A at announcement, G at glide interception, I at impact on ground, position of debris (dotted rectangle), lateral deviation β at impact on ground, vertical descent angle γ. We do not know its position E at encounter with missile. Thin dashed green arrows: hypothetical free fall trajectory (Section II C). Thick blue arrows: actual trajectory (Section II D). Short red arrows: a missile coming from the ground and from the South of the aircraft. (a) Top view, projected on the horizontal plane Oxy. North up, thick black arrow. Angle at impact is known. Free fall would have been a straight line from E to I. Actual trajectory was curved, in comparison to free fall hypothesis E was twice further from I. (b) Lateral view, projected on the vertical plane Oxz. Angle at impact is not known. Free fall would have been a parabola from E to I. Actual trajectory was a parabola too, in comparison to free fall hypothesis its curvature was smaller and its angle at impact was smaller too.

at most $2\ 10^{-3}$, so the modification of the aircraft velocity vector could be at most of order of 2 m/s. In summary, the direction and amplitude of direct momentum transfer from the missile cannot have caused a significant discontinuity in the aircraft velocity vector oriented towards the South nor towards the ground.

A similar calculation could estimate the momentum transfer due to the warhead explosion. As an order of magnitude, we consider the Mistral's 3 kg hexogen-tolite explosive charge which projects around 1500 tungsten beads[19]. Hexogen-tolite yields a detonation velocity $v_d = 8750$ m/s and 1.6 more time energy per kg than a TNT equivalent of $4.184\ 10^6$ J[20]. The explosion energy was thus of order of $2\ 10^7$ J; part of it was converted in kinetic energy E_c of air (shock wave), missile fragments and tungsten beads (of total mass m_t). With $E_c = m_t v_d^2/2$, the characteristic momentum was at most $m_t v_d = 2E_c/v_d = 2 \times 2\ 10^7\ /\ 8750 = 4.6\ 10^4$ kg m/s. Hence, if the momentum transfer had been perfect and purely unidirectional, the aircraft velocity change could have been of order of 0.5 m/s; in practice it was probably much less.

An evasive maneuver was possible, i.e. if the pilot saw a first missile he could have tried to suddenly change the aircraft orientation in order to prevent a second missile to reach its target. Such kind of avoidance behaviour is delayed first by the pilot reaction, of order or 10^{-1} s[21], and second by the aircraft reaction. Regarding the velocity modulus, over the first second it can vary by a few m/s (Figs. 31, 34 of Ref.[22]).

The above data (Section I B 3) enable us to estimate the average speed between crew announcement A and impact I (Fig. 3). The aircraft covered the distance $x_A - x_I = 37040 - 2160 = 34880$ m, with an accuracy around one mile (i.e. $\pm 5\%$) coming mostly from x_A. Assuming t_I = 20h26'01" ± 11 s, the aircraft covered this distance in a time $t_I - t_A = 274 \pm 11$ s (i.e. $\pm 4\%$ accuracy). This means an average speed of 127 m/s (247 kts) with an accuracy around 6%, assuming the accuracies on distance and time are independent. This speed value is consistent with a Falcon 50

approach phase[23].

However, during the descent the aircraft is expected to have decelerated, hence $\dot{x}_I$ differed from the average speed. For simplicity we assume the deceleration a was constant; note that $\dot{x} < 0$ hence $a = \ddot{x} > 0$. Then the speed and position as a function of time were

$$\dot{x}(t) = a(t - t_A) + \dot{x}_A, \quad (3)$$

$$x(t) = \frac{a}{2}(t - t_A)^2 + \dot{x}_A(t - t_A) + x_A \quad (4)$$

where $\dot{x}_A$ and a are unknown. By eliminating $t - t_A = (\dot{x}(t) - \dot{x}_A)/a$ (Eq. (3)) in Eq. (4), the speed profile as a function of distance was

$$\dot{x}(x) = -\left[\dot{x}_A^2 - 2a(x_A - x)\right]^{1/2} \quad (5)$$

A first constraint on the two unknown $\dot{x}_A$, a is given by Eq. (4) using the known impact position x_I and time t_I. To obtain a second constraint we assume that according to the Aircraft Performance Database[23] the pilot was planning to land by arriving at $x = 1100$ m with a speed 67 m/s (130 kts), so that we could use Eq. (5). Eliminating a from both constraints yields a quadratic equation on $\dot{x}_A$, with two negative solutions $\dot{x}_A = -342.5$ m/s or $\dot{x}_A = -181.5$ m/s. While the former value is irrealistic, and beyond the reach of a Falcon 50, the latter (353 kts) is consistent with aircraft data[23]. It yields $a = 0.397$ m/s^2, which is positive as expected. By propagating the uncertainties on the quadratic equation, we calculate that uncertainties (after rounding) are ± 10 m/s for speed and 30% for a (± 0.012 m/s^2).

Eq. (5) then yields the speed at impact, $\dot{x}_I = -72.7$ m/s (141 kts). As a by-product of Eqs. (3-5) we also obtain that the aircraft intercepted the glide ($x_G = 14446$ m) at time $t_G = t_A + 149$ s, i.e. 20h23'56", which as expected is later than the crew declaration (20h21'42") of the intention to intercept it (Ref.[8] p. 12). It then flew at $\dot{x}_G = -122.5 \pm 10$ m/s (238 ± 20 kts), a value which is consistent with aircraft data[23] but rather high (Ref.[9] p. 106). This might mean that our constant deceleration hypothesis (Eq. (3)) should be slightly corrected, with more deceleration before intercepting the glide (between A and G) and less deceleration later (between G and E). Since we lack information we refrain from entering into these detailed calculations.

B. Lateral deviation after encounter

Since the ground impact is at $y_I \approx -100$ m, it means that after the encounter the aircraft has laterally deviated from its planned trajectory towards the left, i.e. towards the South. Combining the 1994 Belgian report on fragment positions (Ref.[7] p. 5) with their own orientation measurements, French investigators have determined the orientation of the aircraft bounces on the ground as 13.7° from initial aircraft trajectory (Ref.[12] p. 188, 189), i.e. 193.7° from x axis. Based on the rectangle length 145 m and half-width 10 m (Section I B 3) we estimate the accuracy of this angle determination to be $\pm \arctan(10/145) = \pm 4°$. This suggests that when hitting the ground, the aircraft trajectory had deviated laterally by $\beta = 13.7 \pm 4°$ from the initial trajectory. In addition, we do not detect any asymmetry of the fragment dispersion, nor any significant (i.e. larger than 4°) deviation of the fragment dispersion main axis from the aircraft bounces on the ground. This suggests that at the time of impact the aircraft lateral orientation and its center-of-mass velocity direction were parallel.

The deviation towards the left could in principle be explained by an evasive maneuver, off-centered momentum transfer from the missile itself or from the explosion, provided their effect had the correct sign. Quantitatively, to simplify the calculation of the inertia matrix we assimilate the aircraft to a homogenous cross of 18.5 m length and width[18]. We obtain that an instantaneous moment transfer (or "impulse") of about 4.6 10^4 kg m/s directly from the missile or from its explosion (see Section II A) off-centered by 9 m could create an angular velocity after encounter with an order of magnitude of up to 1.5 10^{-1} s^{-1}. This would be enough to make the aircraft turn by 13.7° during its fall.

Other explanations which could have caused the observed deviation towards the left include: larger damages by the missile on the left engine than to the right one, and/or a progressive loss of lift on the left wing due to damages. In fact, Belgian investigators inferred from debris that only the left side of the plane had directly hit the ground, and observed that the left wing was much damaged while the right one was intact: both observations suggested the plane had rolled towards the left (Ref.[7] p. 3).

C. Free fall hypothesis and its inconsistencies

To find the aircraft-missile encounter position x_E, we now discuss where the trajectory after the encounter, projected on the horizontal Oxy plane, met the trajectory before the encounter (Fig. 3a).

As a first approximation, let us examine the unlikely but simplest possible trajectory after the encounter, that of a free fall. If the plane had suddenly deviated towards the left then undergone a free fall without any asymmetry between wings, its trajectory seen from the top, projected on the horizontal Oxy plane, would have been a straight line (Fig. 3a), and seen from the side, in the vertical Oxz plane, would have been a ballistic parabola (Fig. 3b) of vertical acceleration $\ddot{z} = -g = -9.81$ m/s^2.

Extrapolating the fragment dispersion angle (Section II B) would imply the encounter to be situated upstream of the ground impact at $x_E - x_I = (y_E - y_I)/\tan\beta$. Here $x_I = 2160 \pm 20$ m; $y_I = -100 \pm 20$ m; $\beta = 13.7 \pm 4°$, hence $1/\tan\beta = 4.10$ with a confidence interval between 3.13 and 5.85; $y_E = 0$ with an accuracy $\pm 8.7\ 10^{-3}\ x_E$. Altogether, this would yield $x_E - x_I = 410$ m and $x_E = 2570$ m (Fig. 2). Assuming that the accuracy on y_E is $\pm 8.7\ 10^{-3} \times 2570 = 22$ m, and that the above confidence intervals are independent, we can determine the confidence interval of x_E. With $\left(20^2 + 4.10^2\left(20^2 + 22^2\right) + 100^2(4.10 - 3.13)^2\right)^{1/2} = 157$ m and $\left(20^2 + 4.10^2\left(20^2 + 22^2\right) + 100^2(5.85 - 4.10)^2\right)^{1/2} = 169$ m we finally obtain for x_E the interval 2413 to 2739 m.

This would determine the fall duration $D = t_I - t_E$ and the speeds $\dot{x}_E$, $\dot{x}_I$. In fact, Eq. (2) would imply that at encounter, $z_E = z_O + x_E\ \tan\gamma = 1486 + 134 = 1620$ m and $\dot{z}_E = \dot{x}_E\ \tan\gamma$. Eq. (5) would yield that $\dot{x}_E = -74.9$ m/s and $\dot{z}_E = -3.9$ m/s. The vertical trajectory $z(t) = z_E + \dot{z}_E(t - t_E) - g(t - t_E)^2/2$ combined with the impact position I would yield a quadratic equation to find D, which positive solution would be $D = 6.2$ s. The vertical speed at impact would be $\dot{z}_I = -64.7$ m/s.

This free fall scenario seems unlikely for several reasons.

First, while this scenario is built on the correct lateral angle at impact β, it would require a very specific combination of ingredients, see Sections II A, II B. To cause a deviation of 13.7° at 77 m/s, the change in velocity at encounter should have been 18.2 m/s, which is too large with respect to the above estimations (Section II A). Moreover, the change in angular velocity should have been, by coincidence, such that during the free fall duration the aircraft orientation changed by 13.7° too. In addition, in order to explain the sign changes of both the center-of-mass and angular velocities, it seems that the missile or its explosion should have affected the aircraft on its right side (i.e. North side) and near its nose rather than its tail.

Second, between encounter and impact, the air flow around the intact right wing has probably remained laminar for some time, changing progressively rather than discontinuously. The aircraft did probably lose lift on the left wing due to damages, but kept enough lift to partially compensate its weight for a significant time. It means while gliding the aircraft could probably have avoided stalling (Fig. 3b). In fact, pictures of the aircraft debris (Ref.[12] p. 95) show that, as expected before landing and for a speed lower than 98 m/s (190 kts[24]) the pilot had already extended the high lift devices (so-called "flaps"). In this landing configuration, the speed at which a Falcon 50 stalls would typically have been of order 42 m/s (80 knots): the actual speed was above this limit.

Incidentally, we can suggest the following consistency check of our speed estimates. With a wingspan of 18.86 m[18], high lift devices a few tens of centimeters high, i.e. a cross-section S of order of 4 m^2, air density ρ of order of a kg/m^3, and a drag coefficient C_x difficult to estimate but of order of unity, we find the aerodynamic drag $C_x \rho \dot{x}^2 S/2$ was roughly of order of 10^5 N; during the fall, only the right motor functioned, so the aerodynamic drag was only half compensated and the resulting force was of order of $5\ 10^4$ N. The aircraft mass M being of order of 10^4 kg, the longitudinal acceleration was of order of -5 m/s^2, yielding $\dot{x}_I - \dot{x}_E$ of order of -5 m/s, compatible with Section II A.

Third, this value of vertical speed, $\dot{z}_I = -64.7$ m/s, would imply a vertical impact angle $\arctan(\dot{z}_I/\dot{x}_I)$, i.e. $\arctan(64.7/72.7) = 41.7°$, which seems too high to explain the observed bouncing on the ground. A French military investigator observed soon after the crash that no debris was inserted in the ground, that there was no crater for the back part of the plane, and that the fore part had continued its longitudinal movement while creating a furrow; he inferred that only a small part of the plane had been damaged by the missile, the plane had slowed down progressively, and was horizontal at the time of impact (Ref.[6] 8567, p. 12). Belgian investigators noted that, although the ground was soft, the impact crater was shallow: they estimated the aircraft impact angle being at most 20° to the horizontal (Ref.[7] p. 3). UK experts agreed with this estimation and added that aircraft debris would have been expected to be found in the crater if the aircraft had adopted a more vertical descent into soft earth (Ref.[9] p. 8).

All these remarks make this free fall scenario unlikely. We thus consider the free fall figures only as upper bounds for the vertical acceleration and vertical impact angle, and as lower bounds for x_E, z_E, $-\dot{x}_E$ and $D = t_I - t_E$.

D. Estimates of encounter position

Beyond the lower bound determination of x_E (Section II C), we can suggest three determinations, one based on geometry, one based on witness indications, and one mixing both (Fig. 2).

(i) The first determination is based on the geometry of the horizontal trajectory, $y(x)$. If we assume the horizontal trajectory was an arc of circle or, to simplify the calculation, a portion of parabola starting at (x_E, y_E) with a tangent parallel to axis x (Fig. 3a), its equation is $y - y_E = \mathrm{cst}(x - x_E)^2/2$ where $y_E = 0$ and x_E is unknown. The place of the

ground impact is known, $(x_I, y_I) = (2160, -100)$, and the tangent angle at the impact is known, $(dy/dx)_I = \tan\beta$. One finds that $x_E - x_I = 2y_I/\tan\beta = 820$ m. This is twice the value it would have in a free fall, and its confidence interval is twice as large (see Section II C). This yields $x_E = 2160 + 820 = 2980$ m, with confidence interval between 2666 and 3318 m.

(ii) The second determination is based on witness indications. Witnesses placed at the airport had a good visibility on the aircraft during its descent, but their axis of view was parallel to axis x: their estimations of x_E were widely spread (we find a distribution of values from 2000 m to 4200 m with a median around 3100 m). Conversely, witnesses looking perpendicularly, e.g. placed at the North and looking South, could better determine x_E. If we compile their indications, at the time of encounter the aircraft was flying over the Nyarugunga district of the Kanombe hill (see also Ref.[10] p. 91), which we translate quantitatively into $x_E \approx 2900 \pm 400$ m.

(iii) The third determination uses both the aircraft speed we have found, and the fall duration $D = t_I - t_E$. We do not know D, since Section II A does not estimate it and Section II C only provides a lower bound of 6.2 s. We thus turn to indication *F–2*. According to it, the duration D of the fall was not longer than 15 seconds. Assuming rather arbitrarily that $D = 12 \pm 3$ s, using $\dot{x}_I = -72.7 \pm 10$ m/s (Section II A), and since $\dot{x}$ only varied by a few percents between E and I (Eq. (5)), we obtain $x_E = x_I + D\,\dot{x}_I = 2160 + 872 = 3030$ m, with an accuracy around ± 300 m.

In summary, the three determinations of x_E are: (i) 2980 m (confidence interval 2666 to 3318 m); (ii) 2900 ± 400 m; and (iii) 3030 ± 300 m. The average is 2970 m and the confidence interval 2629 to 3318 m (Fig. 2). It is compatible with the lower bound, $x_E > 2570$ m. Since the confidence interval is almost symmetrical (-341 m, +348 m), for simplicity in all calculations that follow we symmetrize it and use $x_E = 2970 \pm 345$ m. As discussed in Section V B 1, this value affects several other values calculated below (Table III).

This implies that $z_E - z_O = x_E\ \tan\gamma = 0.052 \times 2970 = 154$ m while the accuracy on x_E is 345 m, that on $\tan\gamma$ is $8.7\ 10^{-3}$, and assuming they are independent yields an accuracy on $z_E - z_O$ of ± 31 m. Hence the aircraft had almost completed its descent and in terms of absolute altitude, $z_E = z_O + 154 = 1639 \pm 31$ m; laterally, $y_E = 0$, with an accuracy of $8.7\ 10^{-3} x_E = 26$ m. Eq. (5) yields the aircraft speed at encounter, $\dot{x}_E = -77.1$ m/s (150 kts), with an accuracy that we roughly estimate to be ± 10 m/s. We also retain a vertical speed $\dot{z}_E = \dot{x}_E\ \tan\gamma = -4.0 \pm 0.5$ m/s. We can at last obtain a refined estimation of the fall duration $D = 11 \pm 2.5$ s. We check it is compatible both with the lower bound 6.2 s (Section II C) and the upper bound 15 s (*F–2*). This fall duration, for a parabolic vertical trajectory, would yield a vertical acceleration 3.06 ± 1 m/s^2: in practice, this value is an average over the trajectory, since the vertical acceleration might have varied due to the air drag on the aircraft. Neglecting this higher-order variations, we find a vertical speed at impact -37.7 m/s (confidence interval 29.3 to 43.7 m/s) and a vertical angle at impact 26.1° (confidence interval 21.3 to 30°); the lateral angle at impact being $\tan\beta = 13.7°$, the lateral speed $\dot{y}_I$ was of order of $\dot{x}_E\ \sin\beta = -18.3 \pm 2.3$ m/s. We thus confirm that the free fall figures (Section II C) were upper bounds for the vertical acceleration and vertical impact angle, and lower bounds for x_E, z_E, $-\dot{x}_E$ and $D = t_I - t_E$. We again refer the reader to Table III to keep track of these results.

III. LAUNCHING POSITION

Many witnesses were assertive that the launching was at Kanombe military camp or surroundings and excluded Masaka; conversely, many other witnesses were assertive that it was Masaka hill or surroundings and excluded Kanombe. In fact, determining the position L from where the missiles were launched from is a two-dimensional problem. It can be solved by combining witness indications of either distances ("trilateration", Section III A) or directions ("triangulation", Section III B).

A. Trilateration, using distances

In principle, witness indications regarding distances could be combined to determine L ("trilateration"), and there are three such categories of indications which involve geometry or physics. In practice, these three categories are difficult to use quantitatively. In addition, some witness do not explain how they estimate distances.

First, sound amplitude could provide a distance information. One mission of the acoustics expert was to determine how the sound amplitude decreases with distance (Ref.[12] p. 224). His conclusion was that the missile launching sound amplitude was perceived as 160 dB near the launching place, 133 dB at 80 m, 125 dB at 200 m, 104 dB at 2100 m (Ref.[13] p. 18). Since no witness mentioned any loud sound from missile launching (by comparison with the explosion sound coming from the aircraft, unanimously described as loud), and more generally witnesses insisted on the difficulty to identify the causes of noises, one can reasonably exclude that a witness has been close to the launching place; we cannot be more quantitative.

Second, sound propagation too could in principle provide a distance information. Consider a witness placed at W who saw the launching of a missile at L, then later heard it, and measured the time lag δt between the view and the sound. Since the speed of sound c_s is known (Ref.[13] pp. 18-19), and recalling that there is no significant wind which could affect sound propagation (Section I B 3), this could have yielded an accurate estimate of the distance $LW = c_s \delta t$. Unfortunately, no single witness simultaneously fulfilled all these conditions.

Third, three indications *A–1*, *B–1*), (*C–1*, mentioned a specific time sequence: these witnesses have heard a noise before they have seen the upper part of the missile trajectories. In principle, this could indirectly provide an useful information, namely an inequality between the distance LW between launching place and witness, and the distance LE between launching place and encounter: $LW/c_s < LE/c_M$, where c_M is the missile average speed. Equivalently, this inequality can be rewritten as:

$$\frac{LE}{LW} > \mathrm{Ma} \tag{6}$$

where $\mathrm{Ma} = c_M/c_s$ is the missile Mach number; its order of magnitude is 2 (Section IV C). Thus L lies close to W. More quantitatively, since W and E are known, the set of points L obeying Eq. (6) is a circle (Fig. 2) around W, off-centered, with a radius $2WE/3$. In practice, these three indications are not mutually consistent (Fig. 2), and the indicated time sequence lacked stability in time (see Section I A 2) for two witnesses.

Finally, the following three indications provided distance estimates without explaining explicitly how they have obtained them. *D–1* had experience in hearing shootings and suggested a distance between 500 and 1000 m. *E–1* saw the launching at 1000 to 5000 m distance, in the direction of Masaka. *F–1* explicitly stated the launching took place near the factory (called "Guttanit") labeled "*F*" on Fig. 2. At that time the factory was only a 80 m × 40 m rectangle (Ref.[6], 6017) centered at $x = 3660$ m and $y = -870$ m (see below, Fig. 5). Given that this landmark size was less than 100 m and its distance to the closest other landmarks was more than 300 m, we rather arbitrarily attribute to this indication a confidence interval of 200 m. These three indications are not mutually consistent (Fig. 2).

We retain that there are three pairs of distance indications (combined with direction indications whenever available), yielding three different results (Fig. 2). The intersection of *A–1* and *B–1* ("Pair 1") would locate L very inaccurately around the airport, west of E. The intersection of *C–1* and *D–1* ("Pair 2") would locate L at Kanombe, south-west of E. The intersection of *E–1* and *F–1* ("Pair 3") would locate L near factory F, south-east of E. Overall, distance indications lack sources, accuracy, stability in time and consistency.

B. Triangulation, using directions

From tens of visual indications (not shown), we have extracted a subset of 8 indications which obey all the following criteria. First, the witness position should be clearly known. Second, the direction details (whether by words, gesture or drawing) are known with enough accuracy to be used quantitatively. Third, the indication should unambiguously point at the launching L, without confusion with encounter E or impact I. The third criterium happens to exclude all witnesses who place L near I, i.e. at the fence of the President's residence; this creates a negative bias against this point. We represent these 8 indications on a map (Fig. 4). Based on the witness indications (size and distance of the landmarks they indicate, quality of their drawings) we estimate that four of them have a direction accuracy around $\pm 5°$, *E–2*, *F–3*, *G–1*, *I–1*, and the four others around $\pm 10°$, *C–2*, *H–1*, *J–1*, *K–1*.

Consider a witness number k ($k = 1$ to 8), of position W_k with coordinates (x_k, y_k), and who has seen L in a direction $\vec{u}_k = (\cos\theta_k, \sin\theta_k)$. Together, W_k and $\vec{u}_k$ define a straight line, Δ_k. The eight straight lines do not intersect at a single point; finding L by triangulation is thus an overdetermined problem (Fig. 4). We use a minimization method based on the square distances to these lines. A point (x, y) has a distance d_k to Δ_k, i.e. to its orthogonal projection on Δ_k; the square of d_k is:

$$\begin{aligned} d_k^2 &= [-(x - x_k)\sin\theta_k + (y - y_k)\cos\theta_k]^2 \\ &= (x - x_k)^2 \sin^2\theta_k - 2(x - x_k)(y - y_k)\sin\theta_k\cos\theta_k + (y - y_k)^2\cos^2\theta_k \end{aligned} \tag{7}$$

We look for the minimum of the root mean square (r.m.s.) distance:

$$\bar{d^2} = \frac{\sum_{k=1}^{8} w_k d_k^2}{\sum_{k=1}^{8} w_k} \tag{8}$$

Here we introduce the possibility of using weights w_k to take into account the differences in their accuracies. For instance, instead of equal weights ($w_k \equiv 1$), with a weight proportional to the inverse of the confidence interval size the four most accurate witnesses can be assigned a weight twice as large as that of the four less accurate ones. Note that

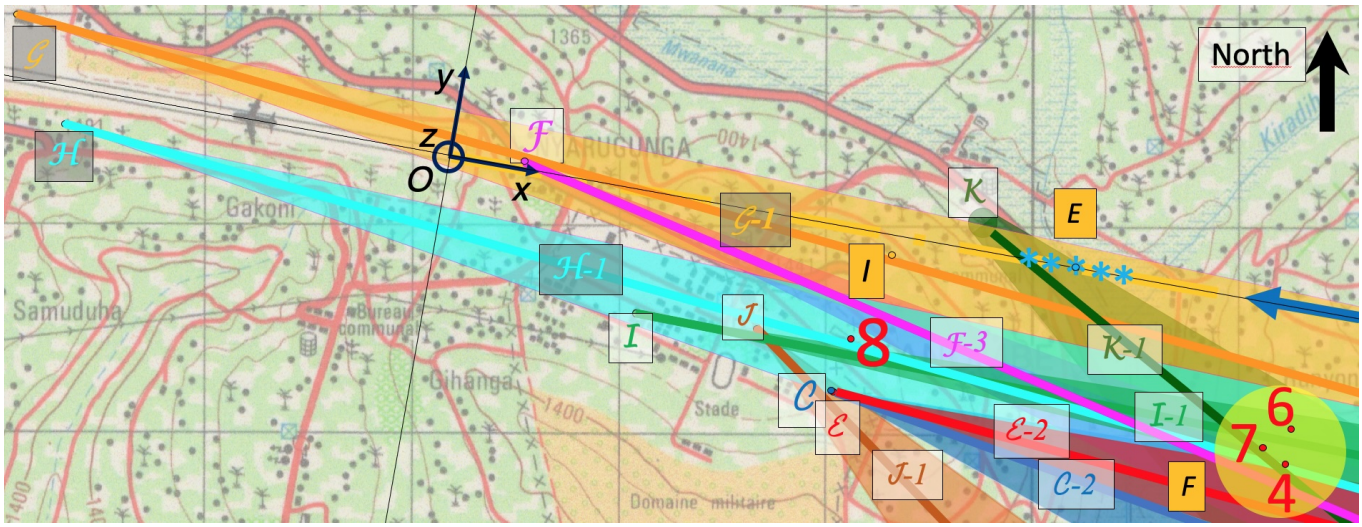

FIG. 4. **Triangulation for missile launching place L based on direction indications.** Geographic North is towards the top (thick black arrow). Scale: grid size is 1 km; the distance between O and E is $OE = 2970 \pm 345$ m. The thick blue arrow is the direction of aircraft arrival. I marks the aircraft impact on the ground (orange dot). The blue dot marks E and the five blue stars ($*$) mark its confidence interval, estimated backwards from the impact data (Section II D). F is the factory. Witnesses are labeled by letters (ex: $\mathcal{A}$), their positions are labeled by coloured dots, their indications are labeled by a number (ex: $\mathcal{A}$*–1*). Directions indicated by $\mathcal{C}$*–2*, $\mathcal{E}$*–2*, $\mathcal{K}$*–1*, are drawn by us according to their indications. Directions indicated by $\mathcal{F}$*–3*, $\mathcal{G}$*–1*, $\mathcal{H}$*–1*, $\mathcal{I}$*–1*, $\mathcal{J}$*–1*, are copied from the drawing by French investigators. The confidence interval for $\mathcal{K}$ position is indicated by the green circle size. Number "8" marks the point minimizing the distance (Eqs. (9,10)) for eight indications when four of them, $\mathcal{E}$*–2*, $\mathcal{F}$*–3*, $\mathcal{G}$*–1*, $\mathcal{I}$*–1*, have a weight twice that of $\mathcal{C}$*–2*, $\mathcal{H}$*–1*, $\mathcal{J}$*–1*, $\mathcal{K}$*–1*. Number "7" marks the point minimizing the distance to the lines drawn by seven witnesses, $\mathcal{J}$*–1* having been excluded); whether with or without weights, the results are indiscernable. Number "6" is for 6 witnesses, with weights, after removal of both $\mathcal{J}$*–1* (outlier) and $\mathcal{C}$*–2* (redundant with $\mathcal{E}$*–2*, and less accurate) and also 5 witnesses after removal of $\mathcal{H}$*–1*, indiscernable. Number "4" is for 4 witnesses after removal of $\mathcal{G}$*–1*. Yellow circle indicates the confidence interval we retain.

$\mathcal{E}$*–2* and $\mathcal{C}$*–2* are redundant: $\mathcal{E}$ and $\mathcal{C}$ were together inside $\mathcal{C}$'s house, estimated the direction based on both noise and light using a compass and landmarks such as trees and their window frame, then immediately recorded the direction on a map. But later, during hearings, $\mathcal{E}$ accurately reported the direction on a map, while $\mathcal{C}$ merely sketched it by hand, thus we attribute a better accuracy and higher weight to $\mathcal{E}$*–2* than to $\mathcal{C}$*–2*.

Minimizing $\bar{d}^2$ (Eq. (8)) amounts to solving the two equations $\partial_x \bar{d}^2 = \partial_y \bar{d}^2 = 0$, i.e.:

$$\sum_{k=1}^{8} w_k \left[2(x - x_k)\sin^2\theta_k - 2(y - y_k)\sin\theta_k \cos\theta_k\right] = 0 \tag{9}$$

$$\sum_{k=1}^{8} w_k \left[-2(x - x_k)\sin\theta_k \cos\theta_k + 2(y - y_k)\cos^2\theta_k\right] = 0 \tag{10}$$

The set of Eqs. (9,10), linear in x and y, has one and only one solution (except when all lines are parallel, which is not the case here).

At first sight, the result we find is suspicious. Weights 2 for the four precise witnesses and 1 for the four others yield $x = +2092$ m, $y = -480$ m, with a r.m.s. distance $\sqrt{\bar{d}^2} = 328$ m. This point (marked by a number "8" in Fig. 4), is compatible with Pair 2 of distance indications (Section III A), and is incompatible with five out of eight direction indications: $\mathcal{E}$*–2*, $\mathcal{K}$*–1*, $\mathcal{C}$*–2*, $\mathcal{J}$*–1* and $\mathcal{I}$*–1*. In particular, the reconstitution of the landscape seen through the window of $\mathcal{C}$'s house (Ref.[12] p. 286), in which both $\mathcal{C}$ and $\mathcal{E}$ were located, shows that Masaka was visible in the middle, while the point "8" would be much too far on the left to be visible through the window by these witnesses.

In such an overdetermined problem, it is advisable to use a robust method to deal with outliers[25]. No method is perfect; choosing the method has an impact on the result. One possibility is to minimize a norm other than the r.m.s. distance $\bar{d}^2$ (Eq. (8)); for instance the average distance $\bar{d}$. For simplicity, we use here the Least Trimmed Squares method[25], which consists in removing one by one the data points in decreasing order of importance. To facilitate the intuitive understanding of the method, we manually implement it as follows.

If we consider $\mathcal{J}$*–1* as the most distant outlier and exclude it, then the resulting position and r.m.s. distance are more consistent and robust to changes in the weight. For instance, with all weights equal, $x = 3948$ m, $y = -747$ m,

while with double weight for the most precise ones we find $x = 3967$ m, $y = -722$ m. The r.m.s. distance is around 212 m in both cases. This point is compatible with the observations of all 7 out of 7 indications (Fig. 4). Some indications have less importance; for instance, the witnesses placed at or near the airport saw both Kanombe military camp and Masaka in the same direction, thus their direction indications (*$\mathcal{H}$–1*, *$\mathcal{G}$–1*) do not discriminate. Removing one by one such indications does not significantly affect the results, which are dominated by the crossing point between *$\mathcal{E}$–2* and *$\mathcal{K}$–1* (Fig. 4). More generally, by testing various weight combinations, we aggregate the results for the launching position L under the values $x_L = +4080 \pm 120$ m, $y_L = -700 \pm 100$ m, with a r.m.s. residual of $\sqrt{\bar{d^2}} \approx 200$ m. Combining the accuracy on L and the r.m.s. residual results in a confidence interval of roughly 300 m (Fig. 4). This is compatible with Pair 3 of distance indications (Section III A).

To summarize this Section, the distance minimization from all eight witness direction indications (number "8" in Fig. 4) is compatible with Pair 2 of distance indications (Section III A), and is incompatible with five out of these eight direction indications. Conversely, the distance minimization of seven out of eight witness direction indications (yellow circle in Fig. 4) is consistent with Pair 3 of distance indications (Section III A) and is consensual between these seven direction indications. This will be further examined in Sections IV A, IV B.

IV. MISSILES

We now examine indications regarding the missile themselves: their launchers (Section IV A), trajectories (Section IV B) and type (Section IV C).

There is a consensus that there was one and only one successful missile. Also, there was no indication that different missiles could have been shot simultaneously from different locations. Both preceding points are important for other Sections. There is no consensus on the two following points which are unimportant for other Sections. Based on ocular and/or auditive indications dispersed in the Rwandan report[10], we determine the number of missiles as distributed in the range 2 ± 1; and the time interval values between missiles as distributed from a fraction of second to many seconds, with a median around two seconds.

A. Missile launchers

A missile launcher is a tube which contains the missile before and during the launching. In normal circumstances, after launching the missile the team packs and removes most accessories, including the launcher. However, here, several witnesses mentioned that two missile launchers have been found. There was no consensus on the existence of these launchers, their number (which was 1 or 3 according to some witnesses), or the finding date (Ref.[10] p. 153-155). We can at least check whether the indications regarding the launcher positions are mutually consistent. We can also check whether these indications are consistent with launching positions independently determined (Section III).

We use a detailed map at scale 1/2500 established by French experts (Ref.[12] p. 60). Witnesses broadly agreed on the finding place, designated using as landmarks either the "Km 19" crossing, "CEBOL", or the Masaka valley (Fig. 5). The Km 19, noted K, is the crossing located at $x = +4140 \pm 10$ m, $y = -820 \pm 5$ m, $z = 1351$ m. CEBOL ("Centre d'élevage de bovins laitiers"), a dairy cattle farming centre also called "Masaka farm" or "The farm", noted C, is at $x = +4520$ m, $y = -1080$ m, $z = 1340$ m. The Masaka valley stretches between these two landmarks, at $z = 1332$ m. One indication mentioned the launchers had been found near the factory, F (*$\mathcal{F}$–4*).

Two indications were more specific (Fig. 5). One was a map with the place where launchers were supposed to have been found drawn just south of the factory (Ref.[6], 8124); from this map we infer $x = +3800 \pm 200$ m, $y = -1200 \pm 100$ m. Rwandan investigators (Ref.[10] p. 154, 156, 157), while doubting the finding was real, mentioned it would have been located "in the marsh", at 300 m from Km 19 and 300 m too from CEBOL. From this indication, we infer two positions (east and west of the KF line), only the west one being near the marsh: it is located at $x = +4100 \pm 100$ m, $y = -1120 \pm 40$ m. Together, these indications would suggest that the missile launchers have been found around $x = +4000 \pm 100$ m, $y = -1130 \pm 30$ m (green cross on Fig. 5). This is on dry land, near the marsh but not in it, and corresponds to $z = 1334 \pm 2$ m.

In summary, the missile launcher indications are mutually consistent. They are also consistent with two out of six witness distance indications (Pair 3, Section III A), consistent with the consensus of seven out of eight witness direction indications (yellow circle, Section III B), and more precise than the latter consensus. Taking into account all these cross-validations, in what follows we retain as a launching position L the point with coordinates $x_L = +4000 \pm 100$ m, $y_L = -1130 \pm 30$ m, $z_L = 1334 \pm 2$ m.

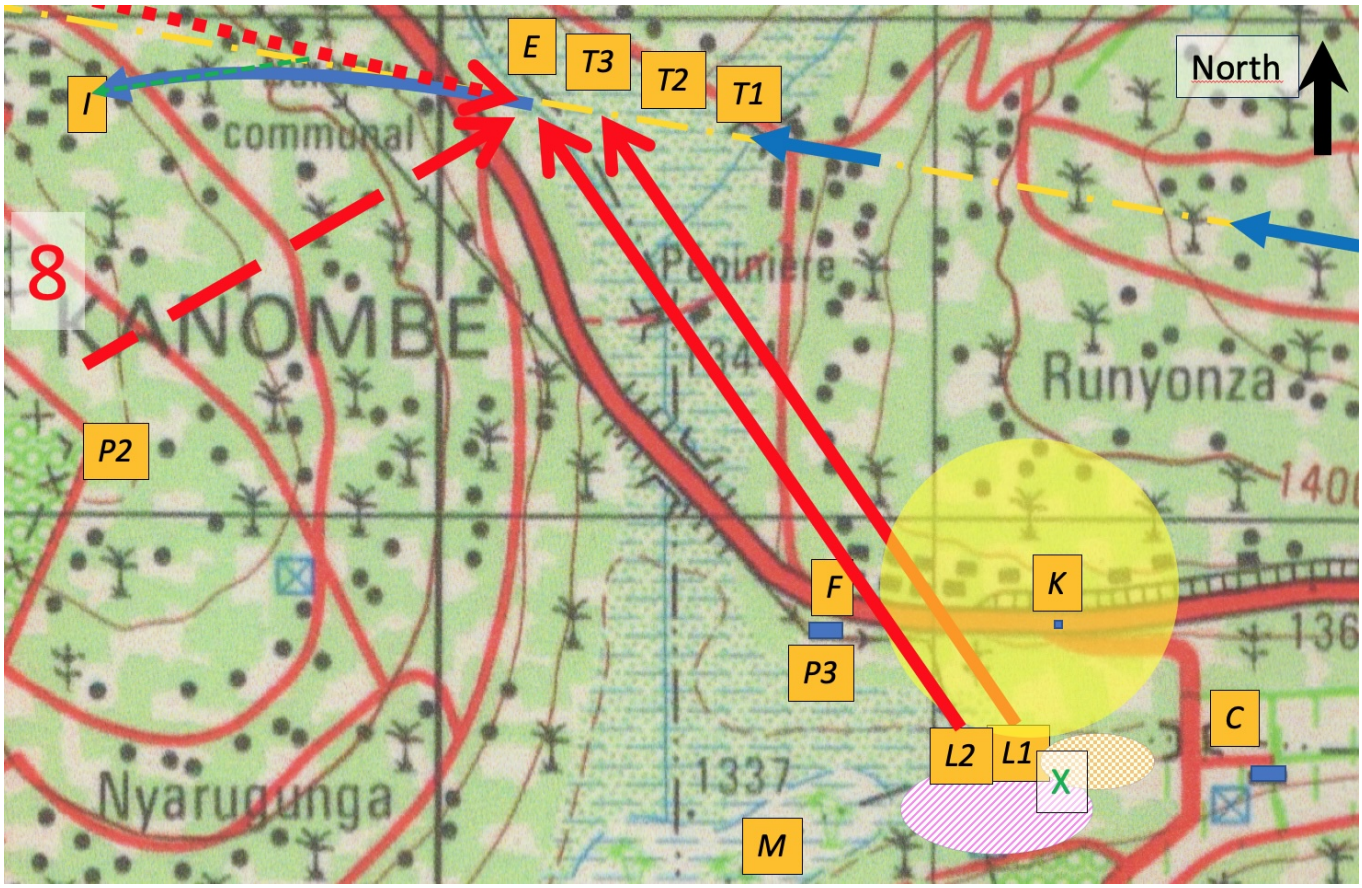

FIG. 5. **Possible missile launching places and trajectories.** Geographic North is towards the top (thick black arrow). Blue rectangles represent the three landmarks F, K and C. The extension of the factory F is that of 1994 (Ref.[12] p. 60). K is the "Km 19" road crossing. C is "CEBOL" or "Masaka farm" or "The Farm". The Masaka valley stretches between these two latter landmarks; M marks the marsh. Scale: grid size is 1 km; the distance between K's center and C's is $KC = 487.5 \pm 2.5$ m. Yellow dash-dotted line: standard aircraft trajectory along the Ox axis. Thin dashed green arrow: hypothetical free fall trajectory (Section II C). Thick blue arrows: actual aircraft trajectory before and after encounter E with missile. For legibility, the confidence interval of E is not drawn (see Fig. 2). I marks the aircraft impact on the ground. Network of lines (red on the original 1988 map[17]): roads (thick), vehicle tracks (thin), paths (dashed). Contour lines (brown on the original map) indicate the altitude, every 100 m (thick), 25 m (thin), 12.5 m (dashed). *Indications on missile launching place (Sections III B, IV A).* Indications where missile launchers have been found: hatch textured purple elongated ellipse (map of Ref.[6], 8124), checkerboard textured orange ellipse (Rwandan investigators, Ref.[10] p. 156-157), and their intersection (green cross). "$P1$" (not shown, off the top left of the map), "$P2$" and "$P3$" mark sound witness indications: Pair 1 intersection of $\mathcal{A}$*–1* and $\mathcal{B}$*–1*), Pair 2 (intersection of $\mathcal{C}$*–1*/$\mathcal{C}$*–2* and $\mathcal{D}$*–1*), and Pair 3 (intersection of $\mathcal{E}$*–1*/$\mathcal{E}$*–2* and $\mathcal{F}$*–1*), respectively (Fig. 2). Number "8" results from eight witness direction indications, including outlier, while yellow circle results from robust witness direction indications without outlier (Fig. 4). *Possible missile trajectory (Sections IV B, IV C).* Red arrows: possible two missile trajectories according to missile launching position based on sound indications P3, robust witness direction indications without outlier, missile trajectory angles and launcher position: "$L1$", "$L2$"; corresponding positions of aircraft: at time of first missile launching ("$T1$"), at time of second missile launching ("$T2$"), when the first missile passed close to the aircraft ("$T3$"), see text. Dashed red arrow: possible missile trajectory according to missile launching position based on sound indications P2, and all witness direction indications. Dotted red arrow: possible missile trajectory according to missile launching position based on sound indications P1.

B. Missile trajectory

We now examine the missile trajectory length, orientation and curvature which, as we discuss below (Section IV C), may have an influence on the missile type determination. Using three-dimensional geometry, we discuss separately the trajectory in the horizontal plane, as would have been viewed from the sky, versus in its vertical plane, as viewed by the witnesses.

From the estimates of missile launching place L (Section IV A) and of encounter position E (Section II D), we infer

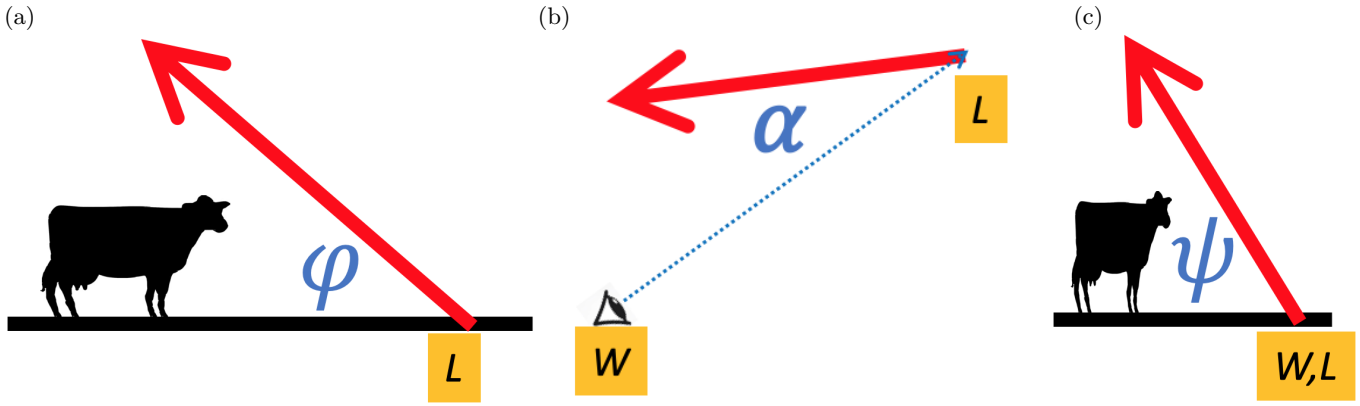

FIG. 6. **Schematic of angle between missile trajectory and horizontal plane.** (a) Actual launching angle φ with respect to the horizontal plane Oxy, seen in the vertical plane containing the missile trajectory. Thick black line: ground, i.e. horizontal Oxy plane; L: launching place; red arrow: initial tangent to the trajectory. (b) Top view projected on the horizontal Oxy plane. W: witness position; dashed blue arrow: the witness' line of view WL; red arrow: the missile trajectory's vertical plane; α: angle between WL and the missile trajectory (in this example $\alpha = 30°$ or $150°$). (c) Apparent missile trajectory angle ψ with respect to the horizontal Oxy plane, as perceived by the witness, along the witness' line of view. In such projection, W and L coincide, and horizontal components of panel (a) elements are affected by a factor $\sin\alpha$ (equal to 0.5 in this example).

TABLE I. **Apparent angle between missile trajectory and horizontal plane.** For definitions and notations see Fig. 6. Values (in degrees) of ψ indicated by four witnesses; confidence interval (minimum; mean; maximum) of α values estimated by us using witness position W, launching position L and trajectory orientation confidence interval (119.8°; 132.3°; 141.9°) with respect to axis Ox; estimates of φ and confidence interval based on ψ, α and Eq. (11).

Indication	ψ	α	φ
$\mathcal{E}$*–3*	60°	(123.8°; 136.3°; 145.9°)	(44.2°; 50.1°; 55.2°)
$\mathcal{J}$*–2*	43°	(126.8°; 139.3°; 148.9°)	(25.7°; 31.3°; 36.7°)
$\mathcal{L}$*–1*	70°	(180.8°; 193.3°; 202.9°)	(02.2°; 32.3°; 46.9°)
$\mathcal{M}$*–1*	45°	(129.8°; 142.3°; 151.9°)	(25.2°; 31.4°; 37.5°)

that the trajectory endpoint coordinate differences $(x_E - x_L, y_E - y_L, z_E - z_L)$ were of order of $(2970 - 4000, 0 + 1130, 1639 - 1334) = (-1030, +1130, +305) \pm (359, 40, 31)$ m. Hence the missile trajectory had a length ℓ_m of order of 1559 ± 362 m, and (after rounding and symmetrizing the confidence interval) an angle within the horizontal plane Oxy with respect to axis Ox of $+132 \pm 11°$ (red arrows on Fig. 5), and an angle (averaged over the whole trajectory) with respect to the horizontal plane Oxy of $12 \pm 4°$. We now examine the consistency of these results with witness indications regarding both angles.

The angle with respect to axis Ox within horizontal plane Oxy lacked stability in time (see Section I A 2) for two witnesses. It was indicated by the first one, $\mathcal{E}$*–1*, as from South-southeast to North-northwest, which we translate as $22.5 \pm 11.25°$ from North axis, or $+122.5 \pm 11.25°$ from Ox axis. The second witness provided a drawing, $\mathcal{C}$*–2*, which we translate as $+156 \pm 10°$ from Ox axis. Together, these indications yield $+139.25 \pm 15°$ from Ox axis. This is consistent with our above estimate of $+132 \pm 11°$ and not with other launching sites situated at the South-West of E.

Another witness ($\mathcal{L}$) was situated in the direction of North-northwest at 20 km distance from E (off the top of Figs. 4, 5), and indicated: "the origin of the two missiles came from the left to head towards the sky towards the right. The angle of the shot was more or less 70 degrees." ($\mathcal{L}$*–1*, Ref.[9] p. 23). Seen from the North-northwest, the indication "from left to right" is compatible with a launching site placed at East side (i.e. North-East, East or South-East of E), not at West side. We assume that "70 degrees" designated the angle ψ with the horizontal plane, as perceived by the witness (Fig. 6), and we now discuss how to exploit such indication.

The actual launching angle φ with respect to the horizontal plane Oxy can be deduced from this perceived one, ψ, using the three-dimensional trigonometric relation (Fig. 6):

$$\tan\varphi = \tan\psi \, |\sin\alpha| \tag{11}$$

The correction which leads from ψ to φ is due to the angle α between the line of view and the missile trajectory vertical plane (α is thus measured within the horizontal Oxy plane). This is an anamorphosis: the vertical component of the

missile velocity vector is unchanged, while its horizontal component is affected by a factor $|\sin\alpha|$. If the witness line of view is perpendicular to the missile trajectory, the witness correctly perceives φ. But in all other configurations, ψ is larger than φ. At the extreme, a witness located in the same plane as the missile trajectory sees it in a vertical plane.

In fact, four witnesses indicated a value for the initial angle, ψ, between the trajectory and the horizontal plane Oxy (Table I). For the four witnesses, we determine α using witness position W, launching position L and missile trajectory orientation $+132 \pm 11°$ with respect to axis Ox. The inaccuracy on α mainly comes from that of the missile trajectory orientation, itself mainly due to inaccuracy on x_E. Since Eq. (11) is non-linear, we separately determine φ_{mean} from the value of α, then φ_{min} and φ_{max} from the $\pm 11°$ confidence interval of α. The average of the four φ values is $\varphi = 36.3°$ with a confidence interval 20.4° to 45°. Independently, we have checked (data not shown) the compatibility between the sign of $\sin\alpha$ and the witness indications that they saw the missile ascending "from left to right" (e.g. *$\mathcal{L}$–1*) or "from right to left" (e.g. *$\mathcal{E}$–1*). With this L position, we find no inconsistency. Note that for alternative launching positions, such as placed at airport by Pair 1 or at Kanombe by Pair 2 (Section III A), we can recalculate the corresponding values of α; we then find incompatibilities both in values of φ and in signs of $\sin\alpha$ (data not shown).

This initial launching angle, $36 \pm 10°$, and the average trajectory angle, $12 \pm 4°$, are compatible if and only if the angle decreased with time, i.e. the trajectory was curved in the vertical plane. This was confirmed by some witnesses, who depending on their position saw this curvature more or less pronounced (we have not detected any inconsistency). The actual trajectory length was thus larger (by around one meter) than the value 1559 ± 362 m determined from endpoints positions.

The other curvature, seen from the top within the horizontal Oxy plane, was not mentioned in the witnesses' indications and has to be inferred from other information. The missile was homing to the aircraft position (Section IV C), with or without a trajectory anticipation procedure. In both cases, since the missile average speed c_M was of order of ten times the aircraft speed at encounter $\dot{x}_E$, the deviation was at most 20° over 1.5 km, hence the radius of curvature would have been at least of order of five km. The trajectory would have been barely curved, and seen from the top the deviation with respect to the straight line would have remained small (Fig. 5).

Assuming there were two missiles launched at two seconds intervals from the position we retain, the aircraft speed at encounter $\dot{x}_E$ and the missile average speed c_M determine the times and aircraft positions "$T1$" when the first missile was launched, "$T2$" when the second one was launched, and "$T3$" when the first missile passed close to the aircraft, respectively around 6, 4 and 2 seconds before E. These points are drawn on Fig. 5, and for legibility we do not draw their confidence interval, which is large: it cumulates the ±300 m inaccuracy on E with that due to our assumptions which is difficult to estimate.

In summary, the indications regarding missile launching angle with horizontal plane (as well as its angle within the horizontal plane, which lack stability in time) are consistent together, as well as with the launching position suggested by two out of six witness distance indications (Pair 3, Section III A), by the consensus of seven out of eight witness direction indications (yellow circle, Section III B), and by missile launcher indications (Section IV A).

C. Missile type

Applying our approach, we look for quantitative arguments to discriminate between surface-to-air weapon types. In 1994, hundreds of types were marketed (Ref.[12] pp. 102-174). These weapon types belonged to one out of these three classes: either non propelled (e.g. machine gun bullets); self propelled but not homing (rockets); or self propelled and homing to the aircraft (missiles), guided by the infrared emission of hot aircraft engine exhaust gases. All three classes travelled at least at 300 m/s over 2000 m distance and 1500 m height. An aircraft flying at 154 m height, 1559 m distance and 77.1 m/s was well within their range. Projectile trajectories were described as luminous (*$\mathcal{N}$–1*): this could be due either to missile flight motor exhaust (Ref.[9] p. 18-19), or to tracer ammunitions. The observed trajectory curvature in the vertical plane excludes rockets; in principle it could be due either to gravity, for bullets, or to guiding, for missile.

However, the trajectory shape provides an argument. If the projectile had been purely ballistic, gravity acceleration of 9.81 m/s^2 would have affected the projectile speed by a few tens of m/s and its height by a few tens of meters, hence would have modestly bent the projectile trajectory. The trajectory shape we have found, with initial launching angle $36 \pm 10°$, and average trajectory angle $12 \pm 3°$, indicates that there was guiding (see an example of missile trajectory curvature on the picture of Ref.[26]). This was confirmed by some witnesses: they saw the trajectories turning and heading towards the plane (*$\mathcal{H}$–2*, *$\mathcal{O}$–1*, *$\mathcal{N}$–1*).

In 1994, the most widespread missile types were Stinger produced in the USA, Strela/Igla/SA/SAM produced in the USSR/Russia, Mistral produced in France. For simplicity, we compare only the specifications of these three types as they were available in 1994. Due to lack of information, we do not detail their many different variants nor their

TABLE II. **Missile trajectory phases.** Quantitative description of the propulsion phase, then the non-propulsion one, for three missile types. Their sources are indicated, either coming from the literature, or from Eqs. (12-18). The value and confidence interval of total missile trajectory length $\ell_m = 1559 \pm 362$ m (Section IV B) propagate to ℓ_{np}, t_{np} and t_m; in the case of Stinger, the non-propulsion phase can vanish, this results in an asymmetric confidence interval represented here as (minimum; mean; maximum).

Quantity	SAM	Stinger	Mistral
Propulsion duration t_p	2 s	3.49 s	2.6 s
	Ref.[9] p. 54	Eq. (12)	Ref.[19]
Propulsion length ℓ_p	686 m	1316 m	1114 m
	Eq. (15)	Eq. (14)	Eq. (15)
Speed at end of propulsion v_p	686 m/s	754 m/s	857 m/s
	Ref.[9] p. 54	Ref.[12] p. 162-167	Ref.[19]
Propulsion acceleration a_p	343 m/s^2	216 m/s^2	330 m/s^2
	Eq. (12)	Ref.[29] p. 3	Eq. (12)
Non-propulsion length ℓ_{np}	873 ± 362 m	(0 m; 243 m; 605 m)	445 ± 362 m
	Eq. (17)	Eq. (17)	Eq. (17)
Non-propulsion duration t_{np}	1.27 ± 0.53 s	(0 s; 0.32 s; 0.8 s)	0.52 ± 0.42 s
	Eq. (16)	Eq. (16)	Eq. (16)
Total duration t_m	3.27 ± 0.53 s	(3.32 s; 3.81; 4.29 s)	3.2 ± 0.42 s
	Eq. (18)	Eqs. (13,18)	Eq. (18)

copies developed in other countries (Ref.[12] p. 108-109).

Missile characteristics such as minimal and maximal shooting distance, speed, or maximal angle with the horizontal plane, do not discriminate between these three types. It was normal for these missiles to be launched far from the horizontal and then bend towards the horizontal (see the trajectory orientations on the picture of Ref.[26]). E.g. for a Mistral the nominal launching range was up to 67°[27]. Also, they had to be launched far enough from their target, since the guiding was operational only above a minimal distance: 500 m for Mistral[27], 1000 m for SAM (Ref.[12] p. 319); as opposed to a non-propelled weapon which would have performed a direct shot and could have been launched from a place much closer to the aircraft trajectory. Finally, the UK experts have used energy dispersive X-ray spectroscopy (EDS) to analyze possible metal fragments both free standing and embedded recovered in 2009 from the debris, but this study was too incomplete to unambigously discriminate the missile type (Ref.[9] p. 32, 108).

In principle, the trajectory length could yield useful indications. Several witness indicated there has been a continuous luminous line from ground to aircraft (e.g. *J–3*, *N–1*); the continuity of the luminous line has been claimed to be a marker of the missile type. French experts considered it as a characteristics of SAM (Ref.[12] p. 321), while UK ones estimated that the SAM trajectory is visible only over the first 1000 m (Ref.[9] p. 18-19); independently, a missile specialist suggested that Mistral trajectory is visible only during the first 2 s while SAM and Stinger trajectories are continuously visible[28].

In order to examine quantitatively this point, we model the trajectory to obtain an order of magnitude for the length and duration of the visible and non visible trajectory phases. Since missile types have variants, we decline to enter into too many details. For instance, to protect the gunner from the flight motor flames, a launch motor ejects the missile at a few meters from the launcher tube before the flight motor ignition begins. This ejection distance is 4 m for SAM (Ref.[12] p. 237), 9 m for Stinger (Ref.[29] p. 3), 12 m for Mistral[27]. For simplicity, we neglect this ejection phase in what follows. We model the trajectory with only two phases. First, a propulsion phase at constant acceleration a_p during which the missile speed increases from 0 to v_p and the trajectory is clearly visible due to flames. Its duration t_p and length ℓ_p are related by the quadratic equations:

$$v_p = a_p t_p \tag{12}$$
$$2\ell_p = a_p t_p^2 \tag{13}$$
$$2a_p\ell_p = v_p^2 \tag{14}$$
$$2\ell_p = v_p t_p \tag{15}$$

Then a non-propulsion phase at constant speed v_p during which the trajectory is less visible. Its duration t_{np} and

length ℓ_{np} obey:

$$\ell_{np} = v_p t_{np} \tag{16}$$

The total missile trajectory has duration t_m and length ℓ_m:

$$\ell_m = \ell_p + \ell_{np} \tag{17}$$
$$t_m = t_p + t_{np} \tag{18}$$

Using the data we collect, we can fill Table II.

Within the above hypotheses, the total trajectory duration is slightly larger than the propulsion phase, so the luminous trajectory appears almost continuous. More specifically, if the trajectory length is at the lower end of its confidence interval, the non-propulsion phase can even vanish for Stinger, so that in this case we use Eq. (18) to fill Table II. In summary, Stinger is more likely to be associated with a continuous luminous trajectory, while for Mistral the non propulsion phase lasts at least 0.1 s (83 m), and for SAM 0.74 s (511 m).

V. DISCUSSION

Hypotheses that can have strong impacts on results include: assuming the aircraft has followed the standard instrument approach procedure; neglecting variations of aircraft acceleration; simplifying the missile trajectory phases; or neglecting aircraft velocity vector changes at encounter with missile. Moreover, methodological choices that can have strong impacts on results include: discarding outliers; deciding between minimization versus inverse inference methods; neglecting variants of each missile type; or ignoring evasive maneuver by the pilot. We now discuss the experts' choices (Section V A) and ours (Section V B), and draw some lessons for pedagogical purposes (Section V C).

A. Discussion of experts' choices

Experts were mandated to make choices and express explicit conclusions. We now discuss how their choices affected their conclusions regarding aircraft trajectory, missile type, and especially launching site. We list their hypotheses and claims for which no justification is provided, or for which the arguments are inconsistent.

1. Aircraft trajectory

Rwandan investigators (quoted by Ref.[9] p. 31) assumed, without providing arguments, $z_E = 1829$ m (6000 ft) and $\dot{x}_E = 77.1$ m/s (150 kts). The French investigators assumed, without providing arguments, $\dot{x}_E = 61$ m/s (120 kts), a discontinuous change at the encounter in the aircraft trajectory angle in the horizontal Oxy plane, and a free fall of the aircraft after the encounter (Ref.[12] p. 178, 189-193), yielding $x_E = 2570$ m and $z_E = 1620$ m. Conversely, our Section II C shows that such assumptions are unlikely, predict an impact angle on ground much larger than observed, and possibly contradict the principles of mechanics; moreover, it provides arguments for gliding during fall, with twice larger longitudinal and vertical distances to impact, twice longer fall duration, half of impact angle, third of vertical acceleration. In turn, these discrepancies affect the determination of missile launching point and trajectory (Section V B 1).

2. Missile type

Rwandan investigators discussed in detail who could have possessed SAMs[10], briefly discussed also who could have possessed Mistrals (Ref.[10] p. 134, 135, 143) and, quoting the Belgian investigators, mentioned an indirect witness indication that it could have been Stingers (Ref.[10] p. 84). Belgian investigators disregarded Mistrals because "it would imply the complicity of authorities of a nation which owns or produces them" (Ref.[7] p. 2). UK experts have focused their material investigations on SAM (Ref.[9] p. 32, 54, 108). French experts excluded Mistrals by classifying them either in the category of "too sophisticated" missiles (Ref.[12] p. 172), or alternatively in the category "too recent" (Ref.[12] p. 137). None of these arguments is discriminant. Regarding the latter argument, since Mistral version 1 was widely available in 1994 (Ref.[12] p. 172; see also Refs.[28,30]) we do not exclude it a priori.

3. Launching site

To determine the launching site experts have established (or have received) a closed list of possible sites. This enabled them to perform calculations, predictions and deductions. Experts have then analyzed the compatibility of each site with witness indications. French experts have assumed, without providing justification, that missile trajectories were straight lines; they have taken pictures of commercial aircrafts landing by day and by night (Ref.[6], 7915) in order to check the lines of sight were clear from each of the listed sites.

Rwandan investigators listed 5 launching sites: 1 in Masaka and 4 in Kanombe, including the President's residence (Ref.[10] p. 158-165). They excluded Masaka based on a sound intensity argument and on $\mathcal{L}$*–1* (Ref.[10] p. 159-160) because without providing justification they interpreted the 70° angle as the angle seen from the top, in the horizontal Oxy plane, between the aircraft and missile trajectories (Ref.[10] p. 62); we consider this interpretation as unlikely (Section IV B).

UK experts have received from Rwandan investigators a list of 3 launching sites, all situated in Kanombe (Ref.[9] p. 15). These UK experts did not add information. More precisely, they looked for contradictions and did not find any (Ref.[9] p. 16-30), thus did not discriminate between these 3 launching sites (Ref.[9] p. 32). French experts, as explicitly specified by their mission (Ref.[12] p. 8), examined 6 launching sites including both Kanombe and Masaka (Ref.[12] p. 224-225). The mission of the acoustic expert specified (Ref.[13] p. 2) that he should answer the following question: which witnesses could have first heard missile launching, then seen the end of missile trajectories? This has had a strong effect on the determination of launching point L position. Facing the differences between the three sound-based indication pairs, French experts have attributed importance to Pair 2, explicitly excluded Pair 1, and ignored Pair 3. This would locate L at Kanombe, south-west of E. We note that this is compatible with the point 8 (Fig. 4) but not with directions indicated by $\mathcal{E}$*–2*, $\mathcal{K}$*–1*, $\mathcal{C}$*–2*, $\mathcal{J}$*–1*, $\mathcal{I}$*–1*. In addition, it is not consistent with missile launcher position (Section IV A), nor with missile trajectory (Section IV B).

B. Discussion of our choices

1. Choices and sensitivity

As opposed to experts, we are not mandated to express explicit conclusions, but we want to examine the arguments. In comparison with experts, our approach offers two advantages.

First, we keep a trace of justifications and consequences of our choices. We chose an open approach, i.e. we avoid any a priori hypothesis on the launching site: the list of indications is compiled, and the launching site is inferred by minimizing the global disagreement with the various indications, possibly weighted (see Section III). We try to make our choices as explicit as possible, to support them with arguments, and to minimize their effects, e.g. by keeping a maximum of data and discarding only obvious outliers using standard procedures. The list of indications we use is subject to biases, for instance when we happen to reject indications placing L at the fence of the President's residence, thus we state it explicitly (Section III A).

Second, we perform consistency checks. Several values that we calculate (Table III) are independent from each other, i.e. a mistake or a rounding of one of these values does not modify the other values. Other values are inter-dependent, for instance a change in x_E propagates and creates a spate of changes, possibly with non-linear effects. As a test of sensitivity and traceability, we round $x_E = 2970 \pm 345$ m as 3000 ± 300 m. Table III shows in tiny italics the corresponding results. We find the launching angle in horizontal plane changes by 2°, in vertical plane by 0.3°, with the average angle in vertical plane unchanged. Missile trajectory length changes by 19 m and the corresponding duration by 0.1-0.2 s. The altitude of encounter changes by 2 m, and at impact the vertical velocity changes by 0.3 m/s, the angle in vertical plane by 0.1°.

2. Likely scenario

In summary, the publicly available information interpreted by our calculations shows that the question of missile launching position is still open.

The three possibilities are, by decreasing order of consistency (Fig. 5): (i) A launching position at the south-east of the encounter (factory - Km 19 - Cebol triangle), see Figs. 4, 5. It is consistent with Pair 3 sound distance indications (which lack justification, Section III A), with the consensus of seven out of eight direction indications after outlier removal using the Least Trimmed Squares method[25] (Section III B), missile launcher position (Section IV A); as well as with the missile trajectory angles within the horizontal plane (which lack stability in time) and with the horizontal planes (Section IV B). (ii) A position at south-west (Kanombe military camp and surroundings). It relies on Pair

2 sound distance indications (one lacking justification and the other lacking stability in time, Section III A). It is consistent with the point 8 (Fig. 4) but not with directions indicated by $\mathcal{E}$–2, $\mathcal{K}$–1, $\mathcal{C}$–2, $\mathcal{J}$–1, $\mathcal{I}$–1 (Section III B). In addition, it is not consistent with missile launcher position (Section IV A), nor with missile trajectory (Section IV B).
(iii) A position at west (airport). It relies only on Pair 1 sound distance indications (which lack accuracy, Section III A).

Based on the most consistent launching position (i), we would obtain the following likely scenario (Fig. 5). Here we have eventually rounded the results to make them as legible as possible. For additional digits, confidence intervals and sources see Table III. For axes and units see Section I B 2.

On April 6th, 1994, the night was dark and the sky was clear. At 20h21'27", the Falcon 50 aircraft was at $x = 37040$ m, $z = 3657$ m, with a longitudinal speed 181.5 m/s (353 kts), and a deceleration 0.397 m/s^2. At 20h24', with a speed 122.5 m/s (238 kts) it intercepted the standard straight trajectory (the "glide") with slope angle 3°. At 20h26', it had almost finished its descent, its high lift devices (so-called "flaps") were extended, it was at $x = 2970$ m, $z = 1639$ m (i.e. 154 m remaining), and flew with a westwards speed 77.1 m/s (150 kts) and downwards speed 4 m/s.

Two self-propelled homing missiles were shot from a point located at $x = 4000$ m, $y = -1130$ m, $z = 1334$ m, i.e. between the factory, the "Km 19" crossing and the bottom of the Masaka valley, close to the marsh. Their type was Stinger, Strela/Igla/SA/SAM, Mistral, or a copy thereof. They were launched at 36° from horizontal, then bent towards a more horizontal trajectory (which average slope was 12°). They covered the 1559 m distance in barely more than 3 s. They arrived with horizontal orientation at 132° from x axis, i.e. three-quarter back (48°) of the aircraft. Their luminous trajectory would have appeared almost continuous if they were Stingers, slightly less so for Mistrals and even less for SAMs.

The aircraft did glide during 11 s, rolling and yawing towards the left, losing lift due to damages, with a left wing reservoir in fire. Its impact on ground was at $x = 2160$ m, $y = -100$ m, $z = 1410$ m, with a westwards speed 72.7 m/s (141 kts), an orientation deviated by 13.7° towards the left, a vertical acceleration 3.06 m/s^2 (a third of the free fall), a downwards speed at impact 37.7 m/s, and a vertical angle at impact 26.1°.

C. Impact for teaching

Each section of this study provides at least one idea of exercise for students. In addition, the impact for teaching is far-reaching, for the following reasons.

The method developed here is in itself a subject to teach. The students can be encouraged to provide data, determine which ones are important to discriminate between alternative models, determine the fields of physics which can feed the reasoning, and prevent circular reasoning while inferring information from whatever existing data. The accuracy discussion can train the students' critical mind, as well as teach methods (e.g. inference, outlier trimming, optimisation) routinely used in several fields of physics research (e.g. in multi-messenger astrophysics, in complex systems studies, or in particle physics[31]). They can learn how the accuracies regarding data propagate to determine results accuracies.

We emphasize the importance of distinguishing hypotheses and methodological choices, and making both explicit and their consequences. Overall, if different choices regarding hypotheses are exposed clearly, students can compare factual arguments and make their own opinion. Students can understand that knowledge is a dynamic process based on trial and errors and that it gets further enriched thanks to explanation, confrontation, and addition of new data.

To conclude, the mission given to the experts is determinant: if the premises are incorrect, even a correct scientific approach can yield incorrect results. We note that in a technical domain, scientific expertise is required to master vocabulary and concept specificities, extract data from disparate sources, interpret and translate them in an unified way, detect which information is missing, suggest explicit hypotheses to compensate. Experts can reduce a difficult problem to a set of separately tractable questions. This makes the problem accessible to undergraduate students, so that method becomes more important than expertise, as we illustrate here. Finally, our study demonstrates the importance and limits of scientific investigation during a judiciary process.

ACKNOWLEDGMENTS

We thank Jacques Morel and Aymeric Givord for maintaining and making accessible the source document database `http://francegenocidetutsi.org`, Guillaume Ancel for technical explanations about missiles, Institut Géographique National (IGN, Brussels) for providing us the 1988 Kigali map and allowing to reproduce it, colleagues from MSC laboratory for stimulating discussions and especially Caroline Derec for critical reading of the manuscript. We welcome feedback on possible mistakes; and in case some are found in the future, we provide details in Table III to ensure their traceability. For the purpose of Open Access, a CC-BY 4.0 public copyright licence

CONFLICTS OF INTEREST

The authors have no conflicts to disclose.

TABLE III. **Results corresponding to scenario with missiles launched from South-East: notations, accuracies and sources.**

See the remarks on rounding and units in Sections I A 2, I B 2. We present here excess digits; for legibility, asymmetric confidence intervals (e.g. for $\dot{z}_I$, Section II D) have been symmetrized. To test the sensitivity to rounding (Section V B 1), values calculated with $x_E = 3000 \pm 300$ m are displayed as tiny figures in italics within brackets.

Name	Symbol	Value	Accuracy	Section	Source
Aircraft before encounter					
Time at crew announcement	t_A	20h21'27"	± 1 s	I B 3	Ref.[8] p. 11
Position at crew announcement	x_A	37 040 m	± 1 852 m	I B 3	Ref.[8] p. 11
" " "	z_A	3 657 m	± 300 m	I B 3	Eq. (2)
Velocity at crew announcement	$\dot{x}_A$	−181.5 m/s	± 10 m/s	II A	Eqs (3-5)
Average deceleration	a	0.397 m/s^2	± 0.012 m/s^2	II A	Eqs (3-5)
Glide slope angle in vertical plane	γ	3°	± 0.01°	I B 2	Ref.[9] p. 106
Position at glide interception	x_G	14 446 m	± 185 m	I B 2	Ref.[9] p. 106
" " " "	y_G	0 m	± 125 m	II	Eq. (1)
" " " "	z_G	750 m	± 125 m	II	Eq. (2)
Time at glide interception	t_G	20h23'56"	± 10 s	II A	by-product of Eqs (3-5)
Velocity at glide interception	$\dot{x}_G$	−122.5 m/s	± 10 m/s	II A	by-product of Eqs (3-5)
Missile before encounter					
Missile number		2	± 1	IV	witnesses
Launching position	x_L	4 000 m	± 100 m	IV A	witnesses with triangulation
" "	y_L	−1 130 m	± 30 m	IV A	witnesses with triangulation
" "	z_L	1 334 m	± 2 m	IV A	Ref.[12] p. 60
Launching angle in horizontal plane		132° *(130)*	± 11° *(10)*	IV B	geometry
Launching angle in vertical plane	φ	36.3° *(36)*	± 12.3° *(11)*	IV B	Eq. (11)
Average angle in vertical plane		12° *(12)*	± 4° *(3)*	IV B	geometry
Trajectory length	ℓ_m	1 559 m *(1 540)*	± 362 m *(316)*	IV B	geometry
Trajectory duration: if SAM	t_m	3.27 s *(3.25)*	± 0.53 s *(0.44)*	IV C	Table II
" " if Stinger	"	3.8 s *(3.79)*	± 0.49 s *(0.4)*	IV C	Table II
" " if Mistral	"	3.2 s *(3.1)*	± 0.42 s *(0.35)*	IV C	Table II
Aircraft-missile encounter					
Position of encounter	x_E	2 970 m *(3 000)*	± 345 m *(300)*	II D	geometry and witnesses
" " "	y_E	0 m	± 20 m	II D	Eq. (1)
" " "	z_E	1 639 m *(1 641)*	± 31 m *(30)*	II D	Eq. (2)
Aircraft velocity at encounter	$\dot{x}_E$	−77.1 m/s	± 10 m/s	II D	Eq. (5)
" " " "	$\dot{y}_E$	0 m/s	± 0.5 m/s	II D	Eq. (1)
" " " "	$\dot{z}_E$	−4 m/s	± 0.5 m/s	II D	Eq. (2)
Aircraft impact on ground					
Time of encounter and impact	t_E, t_I	20h26'01"	± 11 s	I B 3	Ref.[8] p. 12, 13
Fall duration $t_I - t_E$	D	11 s	± 2.5 s	II D	geometry and witness
Fall vertical acceleration	$\ddot{z}$	−3.08 m/s^2	± 1 m/s^2	II D	geometry and velocity
Position at impact	x_I	2 160 m	± 20 m	I B 3	Ref.[12] p. 188, 192
" " "	y_I	−100 m	± 20 m	I B 3	Ref.[12] p. 188, 192
" " "	z_I	1 410 m	± 2 m	I B 3	Ref.[12] p. 188, 192
Velocity at impact	$\dot{x}_I$	−72.7 m/s	± 10 m/s	II A	Eq. (5)
" " "	$\dot{y}_I$	-18.3 m/s	± 2.3 m/s	II D	geometry and velocity
" " "	$\dot{z}_I$	-37.7 m/s *(38)*	± 7.2 m/s *(7)*	II D	geometry and velocity
Angle at impact in vertical plane		26.1° *(26.2)*	± 4.8° *(5)*	II D	geometry
" " " in horizontal plane	β	13.7°	± 4°	II B	Ref.[12] p. 189

* francois.graner@u-paris.fr
† stefano.panebianco@cea.fr

[1] Cross, R., "Forensic Physics 101: Falls from a height", *Am. J. Phys.* 76, 833-837 (2008), <https://doi.org/10.1119/1.2919736>
[2] Sharma, M., "Fundamental Physics used in Forensics", *Forensic Sci. Add.. Res.* 2020, 5, FSAR.000606.2019, <https://doi.org/10.31031/FSAR.2019.05.000606>
[3] Feder, T., "Physicists in forensics - From faulty products to murder, physicists help figure out what really happened", *Phys. Today* 62, 20-22 (2009), <https://doi.org/10.1063/1.3099569>
[4] Pregliasco, R. G. and Martinez, E. N., "Gunshot Location Through Recorded Sound: A Preliminary Report", *J. Forensic Sci.* 47, 1309-1318, 2002, <https://doi.org/10.1520/JFS15566J>
[5] International Organisation of Legal Metrology (OIML), *Guide to the expression of uncertainty in measurement - Part 1: Introduction*, 2023, <https://www.oiml.org/en/files/pdf_g/g001-gum1-e23.pdf>
[6] *Instruction concernant l'attentat du 6 avril 1994 à Kigali*, Tribunal de Grande Instance de Paris, 15 February 2022 (in French), <https://francegenocidetutsi.fr/fgtarchives.php>
[7] Smeets, P. and Paque, J. *Rapport d'enquête, Sinistre aérien du 06 avr 94 à Kigali - Falcon 50*, Note Auditorat Militaire N° 02.02545W94/Cab 8, 1st August 1994 (partly in French and partly in Dutch), <https://francegenocidetutsi.fr/fgtarchives.php>, 7154.
[8] Plantin de Hugues, P. *Rapport d'expertise*, Tribunal de Grande Instance de Paris, 10 April 2002 (in French), <https://francegenocidetutsi.fr/fgtarchives.php>, 6036
[9] Warden, M.C. and McClue, W.A. *Investigation into the crash of Dassault Falcon 50 registration number 9XR-NN on 6 April 1994 carrying former President Juvenal Habyarimana*, Defence Academy of the United Kingdom and Cranfield University, 27 February 2009 (exists in english and in French; page numbers here refer to the English version), <https://francegenocidetutsi.fr/documents/cranfield-en.pdf>
[10] Mutsinzi, J. *et al.*, *Report of the Investigation into the Causes and Circumstances of and Responsibility for the Attack of 06/04/1994 against the Falcon 50 Rwandan Presidential Aeroplane, Registration Number 9XR-NN*, Republic of Rwanda, 20 April 2009 (exists in three languages; page numbers here refer to the english version), <http://mutsinzireport.com>
[11] Mutsinzi, J. *et al.*, *Video Analysis of Habyarimana Plane Crash*, 11 January 2010, <https://www.youtube.com/watch?v=0bRJbPL1d3Y>
[12] Oosterlinck, C. *et al.*, *Rapport d'expertise. Destruction en vol du Falcon 50 Kigali (Rwanda)*, Tribunal de Grande Instance de Paris, 5 January 2012 (in French), <http://francegenocidetutsi.org/rapport-balstique-attentat-contre-habyarimana-6-4-1994.pdf>
[13] Serre, J.-P. *Rapport complémentaire en acoustique*, Tribunal de Grande Instance de Paris, 3 January 2012 (in French), <https://francegenocidetutsi.fr/documents/RapportExpertAcoustiqueJanvier2012.pdf>
Annexes A to E, <https://francegenocidetutsi.fr/documents/AnnexesRapportAcoustique05012012.pdf>
[14] Rwanda Civil Aviation Authority, *HRYR Aerodrom chart ICAO - Kigali, Rwanda*, 25 January 2024, <https://rac.co.rw/eAIP%20Rwanda/1ST%20EDITION_2024_01_25>
[15] Flight Safety Foundation *Approach-and-landing Accident Reduction Tool Kit - Briefing Note 7.1 - Stabilized Approach*, p. 134, table 1, point 8, <https://flightsafety.org/wp-content/uploads/2016/09/alar_bn7-1stablizedappr.pdf>
[16] Civil Air Navigation Services Organisation (CANSO), *Unstable Approaches ATC Considerations*, Appendix A, p. 15, <https://www.icao.int/safety/RunwaySafety/Documents/Unstable%20Approaches-ATC%20Considerations.pdf>
[17] Institut Géographique National de Belgique & Service de cartographie du Rwanda, Rwanda map, serie Z 721, sheet 17, scale 1/50 000, based on 1974 aerial photographs, 1977-1982 updates and 1985 field surveys, edition 1988 (in French), <https://ngi.be/fr/offre/geodonnees-numeriques/cartes-topographiques-standards/>
For an updated map, see Open Street Map, search "Kanombe", <https://www.openstreetmap.org>
[18] Dassault Falcon 50, wikipedia (in French), <https://fr.wikipedia.org/wiki/Dassault_Falcon_50>
[19] SIRPATerre, *Poste de tir Mistral - caractéristiques techniques*, Armée de terre, 2012 (in French), <www.defense.gouv.fr/terre/.pdf>
[20] RDX, wikipedia, <https://en.wikipedia.org/wiki/RDX>
[21] Hick, W.E., "On the rate of gain of information", *Quart. J. Exp. Psychol.* 4, 11-26 (1952). <http://www2.psychology.uiowa.edu/faculty/mordkoff/InfoProc/pdfs/Hick 1952.pdf>

[22] Akdag, R., "Evaluation of fighter evasive maneuvers against proportional navigation missiles", Master thesis, Turkish naval academy, Istanbul (2005)
<https://web.itu.edu.tr/altilar/thesis/msc/AKDAG05.pdf>
[23] Eurocontrol Aviation Learning Centre, *Aircraft Performance Database (only indicative) - FA50 Dassault-Breguet T16*,
<https://contentzone.eurocontrol.int/aircraftperformance/details.aspx?ICAO=FA50&ICAOFilter=FA50>
[24] Dassault Aviation, *Falcon 50 - Airplane Flight Manual*,
<https://www.avialogs.com/aircraft-d/dassault/item/2743-falcon-50-airplane-flight-manual>
[25] Rousseeuw, P. J. and Leroy, A. M., *Robust Regression and Outlier Detection*, Wiley (2005),
<https://doi.org/10.1002/0471725382>
[26] Raytheon, *Stinger missile*; see picture by U.S. Army entitled: *A Stinger missile is launched during a live-fire test at the U.S. Army White Sands Missile Range in New Mexico*,
<https://www.rtx.com/raytheon/what-we-do/integrated-air-and-missile-defense/stinger-missile>
[27] Matra Défense, *Simbad: Système Intégré Mistral Bi-munitions pour l'Autodéfense* (in French),
<http://www.netmarine.net> (consulted August 17th, 2014; no longer online).
[28] Ancel, G., *Rapport d'expertise sur l'assassinat du président Habyarimana, le 6 avril 1994*, blog, 28 January 2018 (in French),
<https://nepassubir.fr/2018/01/28/>
[29] Federation of American Scientists - Military Analysis Network, *MCWP 3-25.10 - Chapter 2 - Stinger Weapon System*,
<https://man.fas.org/dod-101/sys/land/docs/ch2.pdf>
[30] Mistral (missile), wikipedia,
<https://fr.wikipedia.org/wiki/Mistral_(missile)> (in French).
[31] James, F., *MINUIT - Function Minimization and Error Analysis*, Reference Manual, CERN Program Library Long Writeup D506, Version 94.1, CERN, Geneva, 1994,
<https://inspirehep.net/literature/1258343>